CANADIAN
JOURNAL OF RESEARCH

CONTENTS

NATIONAL RESEARCH COUNCIL
OTTAWA, CANADA

TRANSMISSION OF SOUND THROUGH THIN PLATES[1]

By F. H. Sanders[2]

Abstract

The transmission of high frequency sound through plates of brass and nickel has been studied for angles of incidence ranging from 0 to 70 degrees, using effective plate thicknesses varying from one-twentieth of a wave-length to one wave-length. In addition to strong transmissions in the region below the normal critical angle, very sharp and intense transmission maxima are observed at angles of incidence greatly in excess of the critical angle. These transmission maxima fall within three clearly defined angular regions: (i) angles between zero and the critical angle for longitudinal waves; (ii) angles between the critical angle for longitudinal waves and the critical angle for transverse waves; and (iii) angles above the critical angle for transverse waves. In Regions (i) and (ii) the observed data are in satisfactory agreement with a recent theory advanced by Reissner, and good values of the elastic constants are obtained. By an extension of Lamb's theory for flexural vibrations in bars the results in Region (iii) can be interpreted.

Introduction

During the period 1921 to 1929, R. W. Boyle and his co-workers at the University of Alberta carried on an extensive series of experiments on the various aspects of the propagation of sound. In these experiments use was made of the relatively short sound waves obtainable at frequencies ranging from the audible region to some hundreds of kilocycles. In most cases excellent agreement between observed phenomena and classical sound theory was noted. This agreement was particularly marked in the case of the transmission and reflection of sound at normal incidence by plates of solid material immersed in a liquid. In accordance with Rayleigh's theory, it was found that, for normal incidence, maximum reflection occurred when the thickness of the plate was an odd number of quarter wave-lengths, whereas maximum transmission took place through plates an even number of quarter wave-lengths in thickness. When, however, observations were made with plates set at oblique incidence, a number of points were noted that could not be explained in terms of Rayleigh's theory for the general case of transmission of a plane longitudinal wave through a partition of finite thickness. With plates of thickness less than a wave-length, very large transmission ratios were noted at angles of incidence greatly in excess of the critical angle. A large number of observations were made and reported to the National Research Council, Canada, but never published.

In view of these interesting observations, to which the writer's attention was drawn by Dr. R. W. Boyle, it appeared that an investigation of the transmission of sound through thin plates, using modern equipment, would prove of considerable value. The earlier experiments referred to above were carried out by Boyle and Sproule (9) using a tank some fifteen feet in length and wave-lengths of a few centimetres. Measurements of the incident, transmitted, and reflected energies were made by the use of torsion balances. In the experiments to be described, wave-lengths of the order of one millimetre were used and the sound energies measured by means of the light-scattering properties of the sound field.

Since the beginning of this work the results of a study of the elastic properties of solids have been reported by A. Walti (10). He measured the sound energy transmitted through small sections of wedge-shaped plates of glass at frequencies of a few megacycles, using the scattering of light to determine the transmission ratios at various angles of incidence. By the application of a theory proposed by H. Reissner (6) he obtained excellent values for the elastic constants of glass. Walti's experiments were performed at effective plate thicknesses ranging from one-half to three wave-lengths, and all observed effects appear to be substantially in agreement with Reissner's theory. In the present investigation, plate thicknesses ranged from one-twentieth wave-length to one wave-length and strong transmissions similar to those noted by Boyle and Sproule were observed for angles of incidence much in excess of those studied by Walti.

Experimental

The experiments were carried out in a metal tank of dimensions 40 by 24 by 5 in., shown schematically in Fig. 1 (a). These relatively large dimensions were employed in order that reflections from the walls of the tank would be eliminated by absorption in the liquid medium. The source of ultrasonic vibrations was a circular X-cut quartz crystal, 38 mm. in diameter, excited by a push-pull oscillator at frequencies of 1.90, 3.18, 4.43 and 5.65 megacycles. The theoretical angle of divergence of the sound beam was very small, amounting to less than one degree at the lowest frequency employed. Bär (2) and others have pointed out that, because of transverse vibrations in the quartz, a circular or square crystal does not oscillate entirely as a simple piston-membrane, and, accordingly, the field near the crystal does not consist entirely of plane waves propagated in a direction normal to the face of the crystal. At a small distance from the source, however, it can be shown by means of the Hiedemann (1) method that the nature of the sound field approaches very closely to a simple plane wave. In the present work the plate whose transmissions were being studied was located at a distance of 15 cm. from the crystal, well beyond the doubtful region.

The plates studied were of nickel and brass, 2 in. wide by 4 in. long, and ranged in thickness from 0.004 to 0.025 in. for brass and from 0.001 to 0.025 in. for nickel. These plates, specially supplied through the kindness of Anaconda American Brass Limited, New Toronto, and Messrs. Peckovers

Limited, Toronto, were of uniform composition and had been similarly treated for the full range of thicknesses.   In the experiments the plate being studied was rigidly held in a brass frame that could be set at any desired angle with respect to the direction of incidence of the sound beam.   Angles of incidence could be read directly on an external scale to one-quarter of a degree.
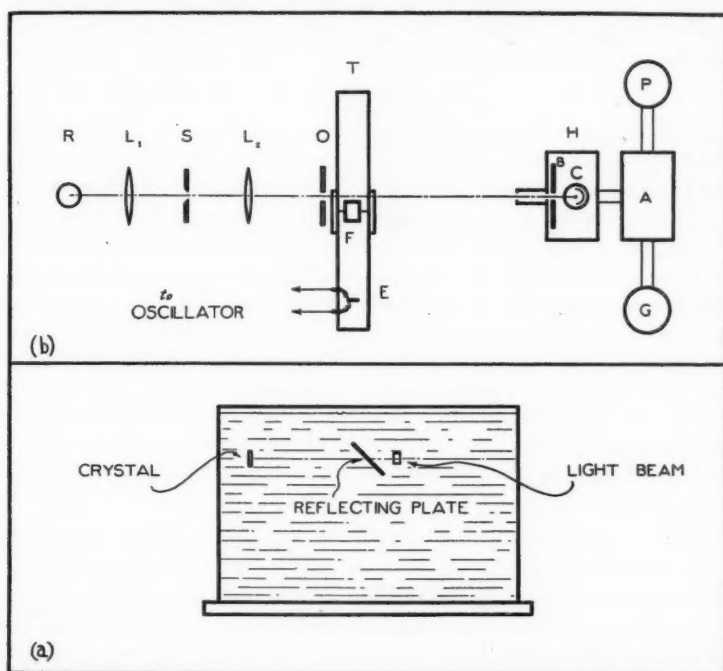
Fig. 1.   (a) Schematic diagram of tank showing relative positions of crystal, plate, and light beam.   (b) Schematic diagram of optical and electrical arrangements.

The intensities of the incident and transmitted sound energies were measured by the scattering of a beam of light that passed normally through the centre of the sound field at a distance of about five centimetres from the axis of the plate holder.   Fig. 1 (b) shows the optical and electrical arrangements. Light from the ribbon-filament lamp, R, is focused by the lens L_1 on the spectrograph slit, S, and the image of this slit is in turn brought to a focus by the lens L_2 on the screen, B, some twelve feet distant.   As the ratio of the distances BL_2 to L_2S was about 12 to 1, the deviation from parallelism of the light beam passing through the windows of the tank, T, was negligible.   When the crystal, E, was excited by the oscillator, any sound energy passing through the plate at F produced scattering of the light beam, and the usual diffraction pattern appeared on the screen, B.   This screen was provided with a slit of such dimensions that light from the central diffraction order only could fall

on a photoelectric cell at C. A system of baffles in the box, H, housing the photocell shielded the latter so well that observations could be taken with moderate illumination in the room. The output of the photocell was amplified at A and carried to the galvanometer G. By the use of a potentiometric device, P, connected to the grid of the amplifier tube, the galvanometer could be used as a null instrument; this eliminated errors due to non-linearity of the amplifier characteristic. The photocell was a vacuum type having an excellent linear characteristic for the light intensities used.

The procedure in making the measurements was as follows:

With the frame, F, empty, so that the sound travelled unimpeded from the crystal to the detecting light beam, the potential exciting the crystal was varied in steps from zero to a value producing four or five diffraction orders. For each value of the applied voltage, measured as in earlier experiments (8), the intensity of the central light image was determined by means of the potentiometer, P. Since the intensity of the sound emitted by the crystal is directly proportional to the square of the applied voltage, this provided a calibration curve giving sound intensities in terms of potentiometer readings. The plate to be studied was next inserted in the frame and the incident sound intensity set at a convenient value. The intensity of the transmitted sound was then measured by means of the potentiometer for angles of incidence from zero to about 70 degrees. Since both incident and transmitted intensities were measured at the same point, it was unnecessary to make any correction for absorption in the liquid.

In order to guard against any change in the output of the oscillator, and thus in incident energy, the potentiometer reading was noted from time to time with the plate set parallel to the direction of incidence. As the ratio of potentiometer readings for this position, and for the case where the plate was removed, had previously been measured, any change in the output of the crystal could readily be observed and corrected.

It was found that, at most angles of incidence, practically no sound was transmitted by even the thinnest plates. At certain discrete angles, however, very intense transmissions were noted. By visual observation of the degree of light scattering it was possible to set the angle of incidence at the exact centre of a transmission peak so that maximum values of transmission could be observed. A complete study of both the intensity and location of the transmission peaks was made, at a frequency of 4.43 megacycles, using the brass plates. For brass at the other three frequencies and for nickel at all four frequencies only the location of the peaks, *i.e.*, the angle of incidence for maximum transmission, was measured, using the visual method. Because of the sensitivity of the optical method it was possible to reproduce all settings to one-half degree or better. As a further check on the locations of the transmission maxima, all measurements were carried out in four quadrants. This eliminated any error due to lack of parallelism of the plate and the external pointer indicating the angle of incidence.

The dimensions of the plates were such that, at the lowest frequency employed, the length was of the order of 50 wave-lengths, and the width, 25 wave-lengths. It thus appeared justifiable to regard all plates as effectively infinite in extent and to assume that only the thickness would have any effect on the location and intensity of the transmission maxima. As a further precaution however the frame, F, was replaced by one 4 by 6 in. in extent, and the locations of the transmission maxima were determined for a number of plate thicknesses. In all cases these maxima occurred at angles of incidence identical with those observed for the smaller plates.

The wavemeter used to measure the frequency was checked against equipment of the standard frequency laboratory of the National Research Laboratories, Ottawa, and found to be accurate to better than 0.1%.

Results and Discussion

Six typical curves A, B, C, D, E and F, indicating the results of the intensity measurements on brass plates at a frequency of 4.43 megacycles are shown in Fig. 2. The ratios of transmitted to incident energy are plotted as ordinates, and angles of incidence as abscissae. For a plate thickness of 0.102 mm.
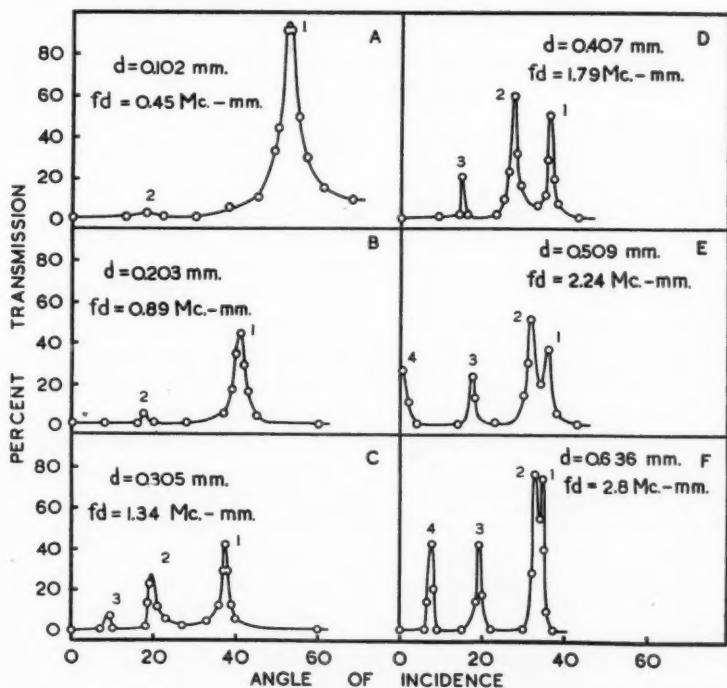

FIG. 2. *Six characteristic curves showing intensities of transmission maxima as a function of angle of incidence for brass plates at a frequency of 4.43 megacycles.*

(0.004 in.) a transmission ratio of 95% is observed at an angle of incidence of 52 degrees (peak 1), while a very faint transmission is observable at 18 degrees (peak 2). At a thickness of 0.203 mm. the position of peak 1 has moved to 41 degrees, while its intensity has dropped to about 45%. The location of peak 2 has not changed perceptibly but its intensity has increased. For a thickness of 0.305 mm. peak 1 has moved still farther to the left, its intensity changing only slightly, whereas peak 2 has moved slightly to the right with a marked increase in intensity. A new peak (3) has also appeared at an angle of incidence of 9 degrees. In the succeeding curves, *D*, *E* and *F*, peak 1 continues to move to smaller angles of incidence while peaks 2 and 3, and finally peak 4, move to larger values. In curve *F*, peaks 1 and 2 have approached each other so closely as to be barely resolvable.

Similar quantitative measurements of both location and intensity of the transmission maxima were carried out for the full range of brass plates, 0.004 to 0.025 in. in thickness. The change in location of the transmission maxima with varying thickness appeared to be of greater immediate interest and more readily adaptable to analysis than the actual magnitudes of the peaks. Measurements of location only were therefore continued on the same set of plates at frequencies of 1.90, 3.18, and 5.65 megacycles using the visual method of observation mentioned earlier.
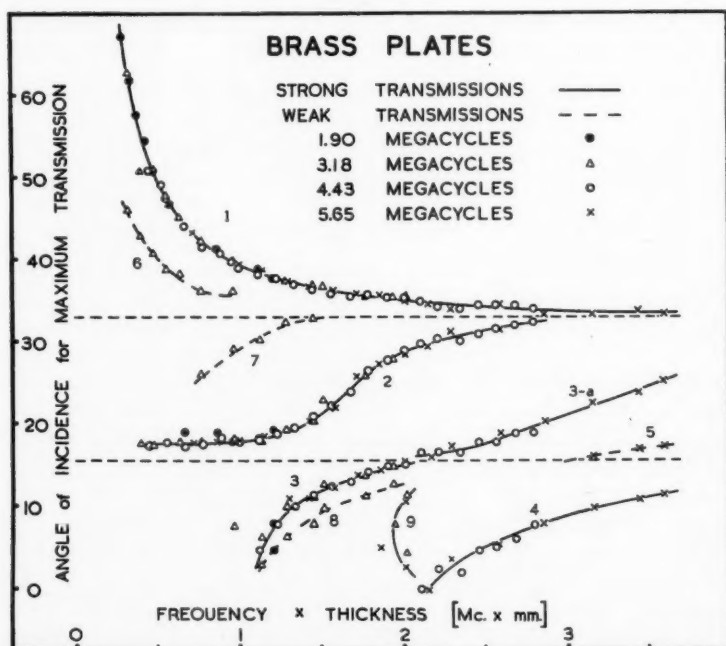

FIG. 3.   *Angle of incidence at which maximum transmission occurs, as a function of the product frequency times thickness, for brass plates at four frequencies.*

Fig. 3 shows the results of the measurements on brass plates at all four frequencies. The angle of incidence at which maximum transmission occurs is plotted as a function of the product fd, frequency times thickness. From the excellent agreement among the data for different frequencies it is evident that the location of a given transmission maximum is determined by the product of these two quantities. The ratio of thickness to wave-length might have been used equally well for the abscissae, but, since this would have involved the velocity of sound in the metal, it appeared advisable to use the two directly measured quantities. The curves marked 1, 2, 3, 3a, and 4 give the locations of the peaks similarly numbered in Fig. 2. The remaining curves, 5, 6, 7, 8, and 9, correspond to maxima of very low intensity. While too weak to be measured accurately by the quantitative method, these peaks were readily detectable by the visual method and could be reproduced to the same accuracy as the stronger peaks. It is to be remarked that the major curves of Fig. 3 are identical in form with those obtained by Boyle and Sproule (9) with glass plates immersed in water.

Examination of these curves shows that they appear to fall into three angular regions. Curves 3, 4, 8, and 9 lie between 0 and about 16 degrees, Curves 2, 3a, 5, and 7 between 16 and about 34 degrees, and Curves 1 and 6 above 34 degrees. Now the velocity of longitudinal waves in an infinite medium is given by the expression

$$w_0 \sqrt{\frac{1 - \sigma}{(1 + \sigma)(1 - 2\sigma)}} ,$$

while the velocity of distortional or transverse waves is

$$w_0 \sqrt{\frac{1}{2(1 + \sigma)}} .$$

In these expressions σ is Poisson's ratio and w_0 is the velocity of longitudinal waves in a long rod. This velocity is a readily measurable quantity and is the value usually quoted in tables. While the values of σ and w_0 vary somewhat with the type of brass, the generally quoted values are 0.35 for σ and 3.4×10^5 cm. per sec. for w_0. The velocity of sound in the ethyl acetate used as the liquid medium in these investigations was measured experimentally by the Hiedemann (1) method and was found to be 1.15×10^5 cm. per sec. From the above figures the velocity of longitudinal waves in brass should be 4.3×10^5 cm. per sec., and that of transverse waves, 2.1×10^5 cm. per sec. These velocities correspond to critical angles of 15.5 and 33.2 degrees respectively. It is thus apparent that the three regions in Fig. 3 correspond to (a) angles between zero and the critical angle for longitudinal waves, (b) angles between the critical angle for longitudinal waves and that for transverse or distortional waves, and (c) angles greater than the critical angle for transverse waves. In the case of the nickel plates, the results for which

are shown in Fig. 4, these three regions are again evident, the critical angles in this case being 11.5 and 23.3 degrees.   In the next section the two lower regions will be considered together and the upper region separately.   The regions *(a)*, *(b)*, and *(c)* will be referred to as B_I, B_{II}, and B_{III} respectively, in accordance with a theory proposed by Reissner (6), to be discussed shortly.
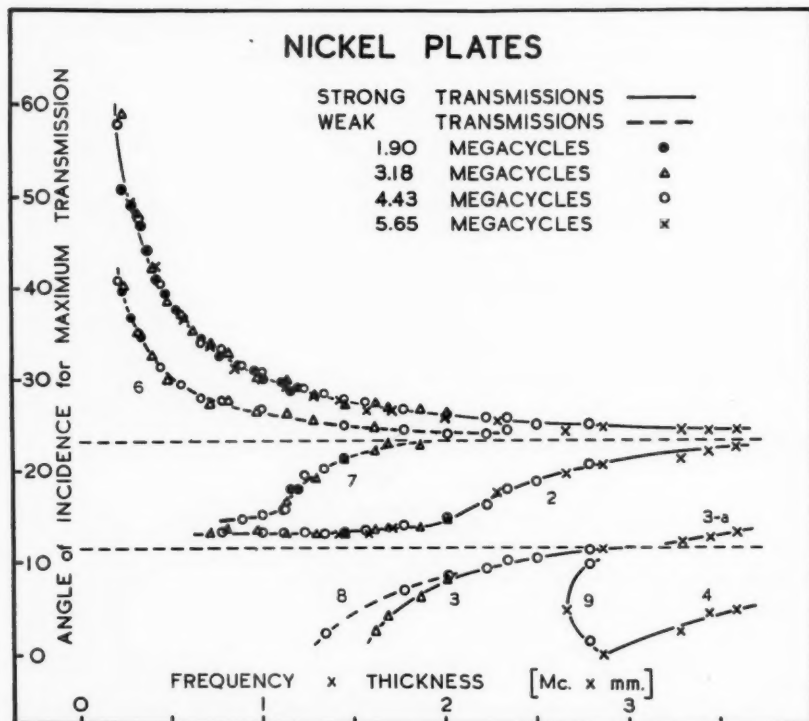
FIG. 4.   *Angle of incidence at which maximum transmission occurs, as a function of the product frequency times thickness, for nickel plates at four frequencies.*

Results in Regions B_I and B_{II} below the Critical Angle for Transverse Waves

It will be noted that Curve 4 of Fig. 3 is the only one showing a definite transmission at normal incidence.   Actually, an intense maximum of transmission was observed for $fd = 2.15 \times 10^6$ mm. cycles per sec.   Rayleigh's theory for the transmission of a longitudinal wave through a plane partition of finite thickness gives the relation:

$$d \cos \theta_1 = \frac{m\lambda}{2}, \tag{1}$$

where d is plate thickness, θ_1 the angle of refraction, λ the wave-length of the disturbance in the plate, and m an integer.   It has been shown by Boyle

and Froman (3) that Equation (1) is quite valid for normal incidence. Placing m equal to unity and θ_1 equal to zero, results in a value for the velocity of the longitudinal waves of 4.30×10^5 cm. per sec., in good agreement with tabulated values. When applied to the case of oblique incidence, however, Equation (1) gives a curve which, although it begins at the point $fd = 2.15 \times 10^6$ and becomes asymptotic to the critical angle for longitudinal waves at large values of fd, deviates widely from Curve 4 of Fig. 3. Furthermore it does not account for the other maxima observed in region B_I.

H. Reissner (6) has quite recently developed a more complete theory for the transmission of sound through partitions of finite thickness at oblique incidence. He considers the case of a plane wave of sound incident on a solid partition with plane parallel walls, and assumes that internal friction may be neglected. The disturbance in the solid medium is regarded as consisting of two pairs of waves, one pair being longitudinal and the other transverse. Each pair is made up of the waves corresponding to the refracted ray and the ray reflected from the internal opposite wall. The system is regarded as a pair of waves because of the change in direction and phase at reflection. Developing this theory, Reissner obtains an expression for the transmission ratio, D, involving the angle of incidence, frequency, plate thickness, and the densities and sound velocities in both media. He shows that while, under appropriate conditions, total reflection of a sound wave entering an infinite medium may occur, this is not necessarily true for a wave entering a body of finite thickness.

In region B_I the application of Reissner's theory is extremely difficult when only the velocity of the longitudinal waves is known. The evaluation of the transverse velocity is much more readily performed in Region B_{II}. Walti (10) has described in detail two methods of determining the latter velocity in Region B_{II} from Reissner's theory. The first of these involves the determination of a certain value θ^* of the angle of incidence such that

$$\sin^2 \theta^* = \frac{w_1^2}{2w_r^2}, \tag{2}$$

where w_1 is the sound velocity in the liquid and w_r is the velocity of transverse waves in the solid. The assignment of this particular value to θ simplifies the computations very materially, so that w_r can readily be evaluated. In the second method described by Walti, w_r is evaluated from the angle of incidence to which the curves in Region B_{II} become asymptotic for large values of the product fd. For further details of these methods the reader is referred to Walti's paper.

The application of the above methods gave the value 2.12×10^5 cm. per sec. for the velocity of transverse waves in brass. With this value of w_r and the value 4.30×10^5 cm. per second for w_d, the velocity of longitudinal waves, obtained from the observations at normal incidence, Reissner's theory can be applied to the observations at any chosen angle of incidence. Actually the computation of the value of fd giving maximum transmission at any given

angle of incidence is extremely laborious, even in Region B_{II}. Consequently, the theory was worked out completely for only a limited number of points. Table I lists a few angles of incidence with the corresponding values of fd, both observed and computed, for which maximum transmission should occur. It is seen that, in Region B_I below the critical angle for longitudinal waves, the agreement between theory and observation is extremely good. Theoretical points exist corresponding to Curves 3, 4, and 9. In Region B_{II} the agreement is good for points on Curves 2 and $3a$ not too near the critical angles, but a noticeable deviation occurs near each of these angles. This same deviation was observed by Walti. It is considerably beyond the limits of experimental error and would appear to indicate certain limitations to the theory. In general, however, the agreement is extremely satisfactory.

TABLE I

Angle of incidence for maximum transmission	Frequency $\times$ thickness					
	First maximum		Second maximum		Third maximum	
	Observed	Reissner	Observed	Reissner	Observed	Reissner
0°	1.05	1.03	2.14	2.15	2.14	2.15
5°	1.14	1.13	1.90	2.07	2.50	2.47
10°	1.32	1.32	1.96	1.96	3.16	3.09
—	—	—	—	—	—	—
18°	1.02	1.31	2.55	2.62		
20°	1.39	1.39	2.86	2.78		
22°	1.55	1.50	3.14	3.00		
24°	1.63	1.63	3.40	3.26		
26°	1.72	1.85	—	3.70		
28°	1.87	2.19	—	4.38		

TABLE II

ELASTIC CONSTANTS—OBSERVED AND TABULATED VALUES

	Nickel		Brass	
	Observed	Tabulated	Observed	Tabulated
Velocity of longitudinal waves in an infinite medium	5.74×10^5		4.30×10^5	
Velocity of longitudinal waves in a rod	4.72×10^5	4.9×10^5	3.47×10^5	3.40×10^5
Velocity of transverse waves	2.90×10^5		2.12×10^5	
Density	8.80	8.8	8.62	8.4 to 8.7
Young's modulus	19.8×10^{11}	21.0×10^{11}	10.4×10^{11}	9.0×10^{11}
Modulus of rigidity	7.4×10^{11}	7.8×10^{11}	3.68×10^{11}	3.5×10^{11}
Poisson's ratio	0.328	0.30	0.339	0.35

The velocities of the longitudinal and transverse waves for nickel were determined in a similar manner and show satisfactory agreement with quoted values. Table II lists the various constants for both brass and nickel as obtained from the observed data, with the corresponding quoted values.

While the elastic constants naturally vary considerably for any given metal, depending on its past history, crystalline structure, etc., the tabulated values are given to indicate the general applicability of the method to the determination of elastic constants.   The horizontal dotted lines in Figs. 3 and 4 indicate the critical angles corresponding to the observed velocities.   It is clear that the curves fall naturally within the three regions defined by these critical angles.

Results in the Region above the Critical Angle for Transverse Waves.

As mentioned in the previous section, Reissner's theory does not require that total reflection should occur for any particular type of wave at the so-called critical angle.   It was shown that in Region B_{II}, above the critical angle for longitudinal waves, the theory explained the observations in a quite satisfactory manner.   When applied to Region B_{III}, however, Reissner's theory does not indicate the presence of transmission maxima at the large angles of incidence actually observed.   Computations of the values of fd for which maximum transmission should occur at angles of 45 and 60 degrees gave no solutions beyond $fd = 0$, although quite intense transmissions were observed at these angles for values of fd near 0.50×10^6 mm. cycles per sec. It would thus appear probable that these transmissions are due to some type of vibration not considered in Reissner's analysis.   The following explanation of the mechanism is proposed.

In Fig. 5 is shown a schematic representation of a plane longitudinal wave in a liquid, incident on a thin plate of solid material at an angle θ.   This longitudinal wave will give rise to a mass flexural vibration of the plate, shown in a greatly exaggerated fashion by the dotted curve.   Now, Lamb (5) has shown that flexural vibrations of this type move with a velocity that is not a constant for the material but varies with the frequency and the plate thickness.   Accordingly, certain angles of incidence will exist for which a plate of thickness d, excited by a longitudinal wave of frequency f in a liquid, will vibrate flexurally with maximum amplitude and will re-transmit a longitudinal disturbance to the fluid.   The wave-lengths of the disturbances in the two media will be related by the equation

$$\lambda_f = \lambda_1 \csc \theta \tag{3}$$
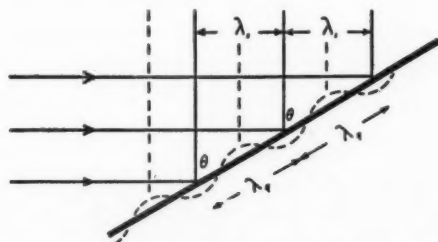

Fig. 5.   *Schematic diagram of a plane longitudinal wave in a liquid, incident on a solid partition at an angle θ.*

and the velocities by

$$w_f = w_1 \csc \theta \qquad (4)$$

where w_1 and λ_1 refer to the liquid and w_f and λ_f to the solid. Lamb's theory for flexural vibrations, while developed for the case of a bar, can quite legitimately be applied[†] under the present experimental conditions, since the velocity of such a flexural vibration is not dependent on the width of the bar. The plate may be regarded as consisting of a series of strips, all vibrating with the same amplitude and phase, and each behaving as a bar of infinite length. For a bar of thickness d, Lamb gives the relation

$$w_f{}^2 = \frac{k^2 \kappa^2}{1 + k^2 \kappa^2} \frac{w_1{}^2}{w_0{}^2} \qquad (5)$$

where κ is the radius of gyration of a section of the bar, equal to $d/\sqrt{12}$ for a rectangular bar of thickness d, k is $2\pi/\lambda_f$ and w_0 is a constant. Combining Equations (4) and (5) gives the relation:

$$\csc^2 \theta = \frac{\pi f d}{6 w_1{}^2} \left\{ \sqrt{\pi^2 f^2 d^2 + 12 w_0{}^2} - \pi f d \right\} \qquad (6)$$

The only unknown quantity in Equation (6) is the constant w_0, and this, according to Lamb, should be the velocity of longitudinal waves in a thin rod. Equation (6) can be shown to give a curve similar to Curve 1 of Fig. 3. For relatively small values of fd the angle θ approaches 90 degrees, while, as fd increases indefinitely, θ approaches asymptotically to the value $\sin^{-1} w_1/w_0$. Equation (6) was applied to the observed data in Region B_{III} and the value of w_0 determined for a number of values of fd. If the theory outlined above were completely valid, w_0 should prove constant. Actually it was found that w_0 decreased consistently with increasing values of fd as shown in Fig. 6 which gives the values for w_0 obtained with brass plates. For small values of fd, w_0 approaches the velocity, $\sqrt{E/\rho}$, of longitudinal waves in a rod, while for large values of fd it approaches the velocity, $\sqrt{\mu/\rho}$, of transverse waves. E is Young's modulus, μ the modulus of rigidity, and ρ the density. This variation appears quite significant. In Lamb's derivation of Equation (5), it is shown that the stress on a section of a bent bar can be regarded as consisting of a transverse shearing force F and a bending moment M. Lamb considers only the case of a bar uniformly bent so that its axis becomes an arc of a circle. Under these conditions the shearing force F vanishes, and it is shown that the bending moment, M, is related to the curvature, R, by the expression:

$$M = \frac{E \omega \kappa^2}{R}, \qquad (7)$$

ω being the area of an element of cross section and κ the radius of gyration of a section of the bar. It thus develops that the quantity w_0 in Equation (5)

† *This point has since been checked by observing the locations of transmission maxima for narrow strips ¼ in. wide by 4 in. long. In all cases, for a given value of fd, transmission maxima occurred at angles identical with those observed with the original plates 2 in. wide by 4 in. long.*

is determined by Young's modulus. When the product fd is small, the wavelength of the flexural disturbance is large compared with the thickness, and the experimental conditions should approach very closely to those imposed by Lamb's theory. That this is so is borne out by the manner in which the experimental values of w_0 approach $\sqrt{E/\rho}$ for small values of fd in Fig. 6. As fd increases, however, there is a considerable deviation from Lamb's conditions owing to the fact that the wave-length becomes comparable with the thickness. The shear forces, previously ignorable, now become very important and eventually become predominant, with the result that w_0 is determined by the modulus of rigidity rather than by Young's modulus. This is strongly supported by the definite manner in which the observed values of w_0 approach the value $\sqrt{\mu/\rho}$ for large values of fd.
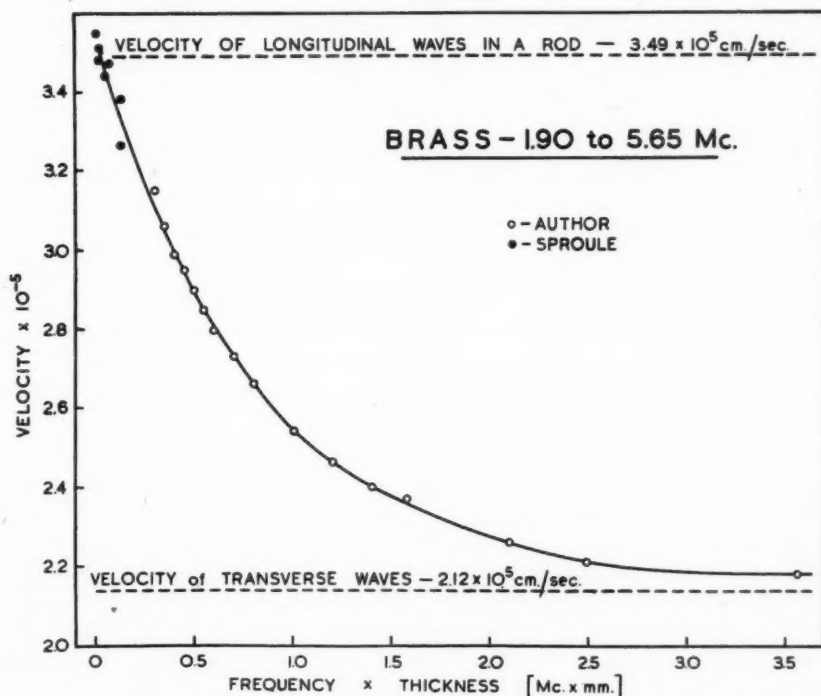

FIG. 6. *Observed values of the quantity w_0 in Equation (6) as a function of frequency times thickness for brass plates.*

The solid points in Fig. 6 at very small values of fd were obtained from some unpublished work performed by D. O. Sproule and kindly supplied by Dr. R. W. Boyle. In Sproule's experiments, the velocity of flexural waves in brass bars was measured at frequencies ranging from 12 to 70 kilocycles by the use of sand figures. The decrease in w_0 with increasing fd is quite evident and serves to corroborate the writer's observations.

The importance of shear forces at high frequencies has been pointed out by Field (4) in relation to the change in velocity of longitudinal waves in solid rods near the fundamental frequency of radial vibration. It was observed by Röhrich (7) that, near the frequency of radial resonance, the longitudinal velocity decreases rapidly, finally approaching and maintaining the velocity of the shear waves. Field has indicated how this phenomenon may be explained by proper consideration of the shear forces.

The theory outlined above was applied to the data obtained with nickel plates in Region B_{III}, and a similar variation in w_0 with fd was noted. In the case of nickel, w_0 varied from the value 4.7×10^5 cm. per sec. for fd small to 2.9×10^5 for fd very large. Comparison with Table II indicates that this variation is from the longitudinal to the transverse velocity, as in the case of brass.

Intensity Measurements

In Fig. 7 are shown the measured intensities of the transmission peaks corresponding to Curves 1, 2, 3, 3a, and 4 of Fig. 3. All peaks should theoretically attain intensities of 100%. Actually it is seen that their intensities vary markedly with thickness. While the values appear rather scattered, particularly in the case of Curve 1, the observations were in most cases reproducible to within a few per cent, and it appears probable that the intensities fluctuate with plate thickness much more than the smooth curves would indicate. In view of the fact that present theoretical analyses are not sufficiently complete to account for deviations from total transmission, it did not
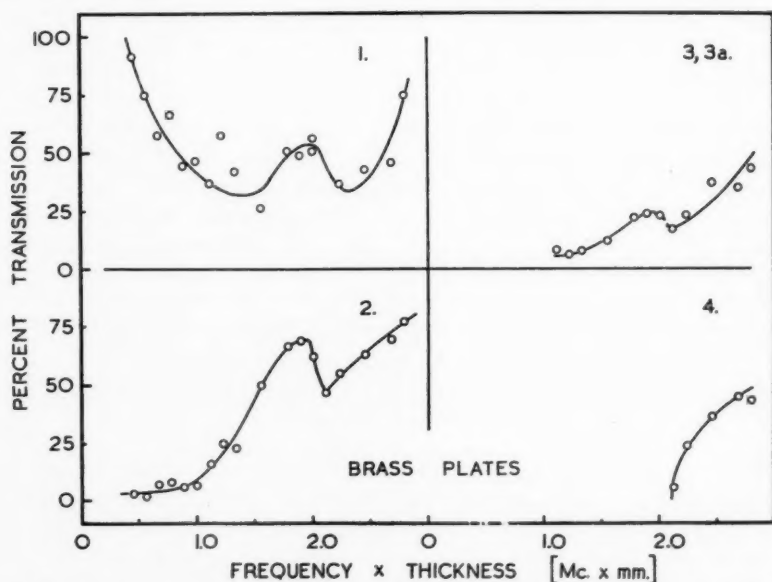

FIG. 7.   *Intensities of the transmission maxima corresponding to Curves 1, 2, 3, 3a, and 4 of Fig. 3, as a function of the product frequency times thickness.*

appear necessary to pursue the intensity measurements beyond the one frequency of 4.43 megacycles.

Other Transmission Maxima

It will be noted that in Figs. 3 and 4 a number of dotted curves (5, 6, 7, and 8) appear. These curves corresponded to very weak transmissions of the order of a few per cent. In spite of their weakness, they were quite definite and consistent in their variation with frequency and thickness and were undoubtedly not due to reflections from the tank walls or to other extraneous effects. In the present state of the theory no explanation for their appearance can be given.

Summary and Conclusions

From the foregoing discussion it would appear that the transmission of sound through partitions of finite thickness can be explained in terms of three different types of vibration occurring in the solid medium. The first is the normal longitudinal or dilatational type of vibration; the second, the transverse or distortional type naturally accompanying the former in an infinite medium; and the third, a mass flexural vibration moving in a direction parallel to the boundaries of the partition. This third type is detectable only for effective plate thicknesses of one wave-length or less. At greater thicknesses the angle at which maximum transmission occurs approaches so closely to the critical angle for the transverse waves that the transmission maxima merge with those due to this type of vibration. Reissner's excellent theoretical analysis describes the phenomena due to the longitudinal and transverse vibrations in a very satisfactory manner, while the indicated extension of Lamb's theory for flexural vibrations appears to account for the transmissions at angles in excess of the critical angle for transverse waves.

Acknowledgments

References

1. BACHEM, CH., HIEDMANN, E., and ASBACH, H. R. Z. Physik, 87 : 734-737. 1934.
2. BÄR, R. Helv. Phys. Acta, 10 : 311-322. 1937.
3. BOYLE, R. W. and FROMAN, D. K. Can. J. Research, 1 : 405-424. 1929.
4. FIELD, G. S. Can. J. Research, 11 : 254-263. 1934.
5. LAMB, H. Dynamical theory of sound. 2nd ed. pp. 122-125. Edward Arnold & Co., London. 1925.
6. REISSNER, H. Helv. Phys. Acta, 11 : 140-145. 1935.
7. RÖHRICH, K. Z. Physik, 73 : 813-832. 1932.
8. SANDERS, F. H. Can. J. Research, A, 14 : 158-171. 1936.
9. SPROULE, D. O. Acoustic reflections and transmissions by the ultrasonic method. Report to the National Research Council of Canada. April, 1929.
10. WALTI, A. Helv. Phys. Acta, 11 : 113-139. 1938.

AN APPARATUS FOR THE DETECTION OF MAGNETIC MATERIALS[1]

By J. S. Johnson[2] and G. S. Field[2]

Abstract

An apparatus for the detection of magnetic materials is described which operates on continuous direct current instead of alternating current or interrupted direct current, as has been the case with previous detectors. This apparatus is highly sensitive and requires very little adjustment. Once installed it can be operated by a non-technician.

Introduction

Various types of metal detectors have been devised using either alternating current or interrupted direct current. They have the inherent difficulty of combining sensitivity with ease of adjustment. Most of these detectors are essentially balanced inductance bridges, and depend for their operation on the disturbance of the balance when a magnetic material is brought into the field of one of the inductance arms of the bridge.

The following is a description of a detector of magnetic materials which works on continuous direct current, and which, having once been set up properly, needs no further electrical adjustments. It was designed to be operated without the assistance of a technician, and to be sensitive enough to detect small objects such as a piece of hacksaw blade or small file.

Description

In Fig. 1, C_1, C_2, and C_3 are coaxial coils large enough to permit a man to walk through them; in the experimental model, 2 ft. 6 in. by 6 ft. 10 in. and spaced 9 in. apart.
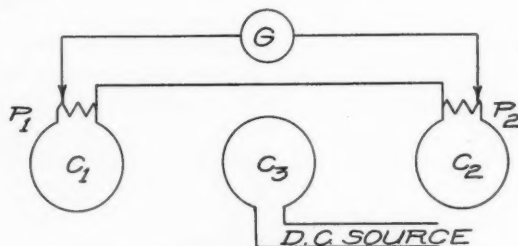

Fig. 1. *Schematic diagram showing coil and galvanometer connections.*

Coil C_3 is energized by a direct current source and serves to produce a relatively high flux density through the pick-up coils, C_1 and C_2, which are connected in series opposition to a medium-sensitivity galvanometer. The

---

potentiometers, P_1 and P_2, are necessary in order to balance out fluctuating magnetic fields, embracing both coils, which are present in most locations in ordinary buildings. Once adjusted, these potentiometers do not need to be touched unless other sources of magnetic disturbance are introduced into the vicinity of the coils.

In Fig. 2 is shown an arrangement that was used to translate the motion of the light beam from the galvanometer mirror to a relay-actuated detector service.
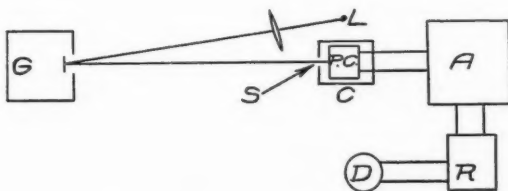

FIG. 2.   *Schematic diagram showing optical system and connections to relay-actuated alarm device.*

Light from the source L passes through a long focus convex lens on to the mirror of the galvanometer, G. It is reflected from the mirror and brought to a focus on a slit, S, in a container, C, surrounding a photocell $P.C.$ This cell is connected to an amplifier, A, whose output is used to operate a relay, R, and hence the alarm device, D.

Operation of Apparatus

When a piece of magnetic material is moved near one of the coils, C_1 or C_2, a change of the flux through the coil occurs. This causes a current to flow through the galvanometer. The resulting motion of the galvanometer mirror shifts the light beam from the slit, S, so that the light no longer falls on the photocell. The drop in current through the cell is amplified by A, and this causes the relay and hence the alarm device to operate.

In an actual installation the photocell and container should be mounted on a rack, so that a drift of the galvanometer mirror can be compensated for by moving the slit. In general this is the only adjustment of the apparatus required while it is in operation.

The metal in an ordinary shoe caused a large deflection of the galvanometer in the experimental model, and the apparatus was sufficiently sensitive to signal the passage of an ordinary hair pin through the coils.

PRESSURE, VOLUME, TEMPERATURE RELATIONS OF ETHYLENE IN THE CRITICAL REGION. II[1].

BY R. L. McINTOSH[2], J. R. DACEY[2], AND O. MAASS[3]

Abstract

The data of a previous publication have been extended. Nine pressure isothermals of the one component system ethylene in the critical region are given. Further evidence of the existence of a two phase system above the temperature of meniscus disappearance as normally determined is presented. The existence of a latent heat of vaporization above this temperature is pointed out. An explanation of the hysteresis of liquid phase density with temperature at constant volume is offered, and a qualitative description of the changes occurring in the transition region of liquid to gas is developed from the experimental evidence.

Introduction

In an earlier paper the authors reported the determination of isothermals of ethylene from $8.92°$ to $9.60°$ C. (2). Unfortunately, an explosion destroyed the apparatus before all the desired data had been obtained. The present paper describes the continuation of these experiments.
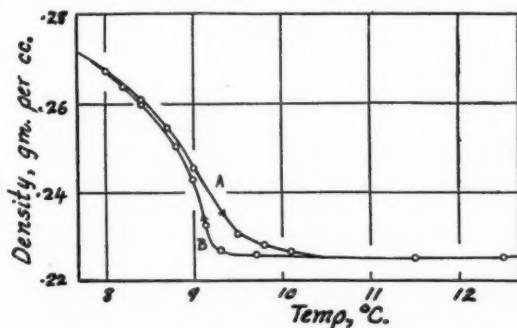

FIG. 1. *Isochore. A. Densities of medium below meniscus on heating above critical temperature. B. Densities subsequently observed during cooling.*

The interest in the work centres about the pressure relations that exist along the A and B curves of a typical isochore (Fig. 1). It was found by Maass and Geddes that the pressures of the A and B curves were identical

at any given temperature for the average density investigated by them (5). Also, the pressure of a heterogeneous system was shown to be the same as that of a homogeneous system at the same average density, obtained by isothermal expansion from liquid densities. The isothermals obtained by Maass and Geddes failed to exhibit any region of density wherein $\left(\dfrac{\partial P}{\partial V}\right)_T = 0$, above the classical critical temperature. The prediction of Harrison and Mayer that such regions should exist, even above the critical temperature, was therefore not corroborated (4). A pertinent criticism by Mayer of this experimental work, in which he pointed out that observations had not been taken at sufficiently minute volume intervals, has led to the construction of an apparatus with which pressure, volume, temperature measurements of a high relative accuracy can be made. For a description of this type of apparatus, and an account of the preliminary measurements made with it, the reader is referred to the earlier paper (2). Added weight was given to Mayer's observation by the work of McIntosh and Maass, which showed that the pressure of heterogeneous systems at 9.80° C. was independent of the mass-volume ratio over an appreciable range of density (6). If the earlier work were to be concordant with this, the isothermals must necessarily exhibit regions even above the critical temperature, where $\left(\dfrac{\partial P}{\partial V}\right)_T = 0$. That such regions are detectable has been shown in the preliminary publication. In the present work the envelope of these regions has been completely traced, and the pressure relations that hold within it have been investigated.

Experimental Results

Nine isothermals from 8.92° to 10.00° C. are given in Table I, and are shown in Fig. 2. The previously published figures are included and the whole

TABLE I

PRESSURE-VOLUME-TEMPERATURE RELATIONS OF ETHYLENE

Exp. vol.	Amount of ethylene, gm.	Specific vol.	Press., atm.	Exp. vol.	Amount of ethylene, gm.	Specific vol.	Press., atm.
Isothermal at 8.92° C.							
2.532	0.716	3.563	49.92	3.271	0.716	4.568	49.45
2.587	.716	3.613	49.73	3.681	.716	5.141	49.46
2.672	.716	3.731	49.54	4.303	.716	6.009	49.38
2.893	.716	4.040	49.45	4.317	.716	6.029	49.34
Isothermal at 9.22° C.							
2.590	0.716	3.617	50.18	2.970	0.716	4.148	49.75
2.613	.716	3.649	50.06	3.284	.716	4.586	49.75
2.655	.716	3.708	49.96	3.666	.716	5.120	49.73
2.715	.716	3.791	49.87	3.876	.716	5.410	49.72
2.794	.716	3.902	49.83	4.006	.716	5.594	49.68
2.830	.716	3.952	49.80	4.174	.716	5.831	49.65

TABLE I—*Continued*

PRESSURE-VOLUME-TEMPERATURE RELATIONS OF ETHYLENE—*Continued*

Exp. vol.	Amount of ethylene, gm.	Specific vol.	Press., atm.	Exp. vol.	Amount of ethylene, gm.	Specific vol.	Press., atm.
Isothermal at 9.42° C.							
2.710	0.716	3.770	50.26	3.300	0.716	4.609	49.99
2.735	.716	3.819	50.15	3.550	.716	4.958	49.97
2.838	.716	3.963	50.06	3.723	.716	5.199	49.94
2.950	.716	4.120	50.02	3.910	.716	5.446	49.90
3.176	.716	4.437	49.99	4.104	.716	5.731	49.85
Isothermal at 9.50° C.							
2.705	0.716	3.777	50.44	2.970	0.716	4.148	50.12
2.722	.716	3.801	50.34	3.235	.716	4.519	50.08
2.762	.716	3.857	50.24	3.455	.716	4.826	50.07
2.789	.716	3.895	50.21	3.624	.716	5.061	50.05
2.829	.716	3.951	50.19	3.857	.716	5.386	49.98
2.908	.716	4.047	50.14	4.197	.716	5.861	49.92
Isothermal at 9.60° C.							
2.695	0.716	3.763	50.52	3.512	0.716	4.891	50.15
2.713	.716	3.775	50.45	3.607	.716	5.037	50.14
2.756	.716	3.849	50.34	3.710	.716	5.181	50.13
2.854	.716	3.986	50.27	3.859	.716	5.389	50.09
3.135	.716	4.378	50.18	4.020	.716	5.614	50.05
3.360	.716	4.692	50.17				
Isothermal at 9.70° C.							
2.823	0.722	3.909	50.42	3.318	0.722	4.605	50.27
2.884	.722	3.994	50.35	3.414	.722	4.729	50.25
2.953	.722	4.090	50.30	3.640	.722	5.041	50.22
3.109	.722	4.306	50.28	3.885	.722	5.381	50.18
3.187	.722	4.414	50.28	4.004	.722	5.546	50.17
Isothermal at 9.80° C.							
2.761	0.722	3.824	50.65	3.066	0.722	4.246	50.40
2.776	.722	3.844	50.61	3.108	.722	4.304	50.39
2.808	.722	3.889	50.56	3.197	.722	4.429	50.39
2.863	.722	3.965	50.50	3.262	.722	4.518	50.38
2.902	.722	4.019	50.47	3.328	.722	4.609	50.37
2.954	.722	4.091	50.44	3.464	.722	4.792	50.34
3.025	.722	4.189	50.42	3.635	.722	5.030	50.32
Isothermal at 9.90° C.							
2.770	0.722	3.837	50.74	3.072	0.722	4.255	50.52
2.807	.722	3.890	50.69	3.132	.722	4.338	50.51
2.854	.722	3.953	50.65	3.224	.722	4.466	50.50
2.923	.722	4.048	50.60	3.302	.722	4.574	50.48
2.961	.722	4.101	50.57	3.512	.722	4.864	50.45
3.030	.722	4.197	50.54	3.737	.722	5.178	50.42

TABLE I—*Concluded*

PRESSURE-VOLUME-TEMPERATURE RELATIONS OF ETHYLENE—*Concluded*

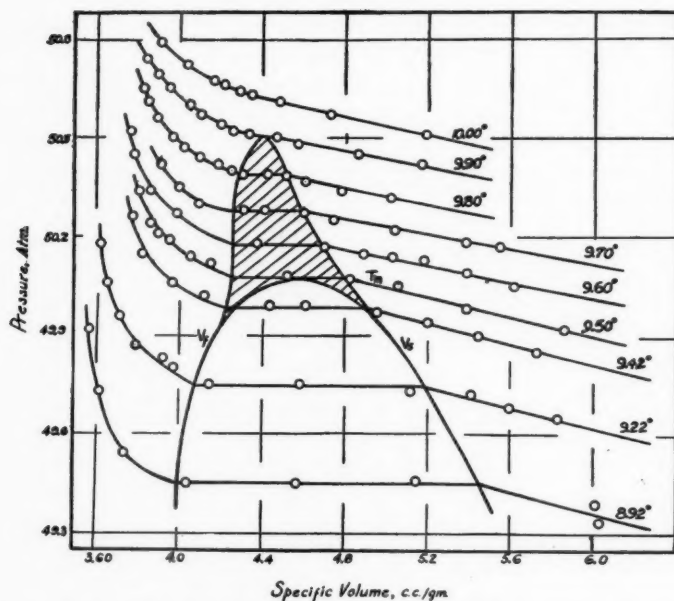| Exp. vol.	Amount of ethylene, gm.	Specific vol.	Press., atm.	Exp. vol.	Amount of ethylene, gm.	Specific vol.	Press., atm.
Isothermal at 10.00° C.							
2.820	0.722	3.905	50.79	3.155	0.722	4.370	50.63
2.913	.722	4.034	50.72	3.236	.722	4.482	50.61
3.005	.722	4.162	50.67	3.396	.722	4.703	50.57
3.045	.722	4.217	50.66	3.750	.722	5.194	50.51
3.083	.722	4.270	50.64				

FIG. 2. *Isothermals. Relation between specific volume and pressure at temperatures in the critical temperature region.*

tabulated in terms of specific volume.   The experimental error in determining the absolute densities is ±1%.   In order to show that the contiguity of the curves obtained with the two assemblies used is real, the isothermal at 9.22° C. was repeated.   The agreement was exact.

Pressure measurements along the *A* and *B* curves of isochores of three different mean densities were made, in order to determine the relative stabilities of the heterogeneous and homogeneous systems under a variety of conditions. These results are shown in Table II.

TABLE II
PRESSURE MEASUREMENTS OF HETEROGENEOUS SYSTEMS

Temp., °C.	Pressure, atm. density = 0.2046 gm. /cc.	Pressure, atm. density = 0.2109 gm. /cc.	Pressure, atm. density = 0.2270 gm. /cc.	Pressure of isothermals
Heating				
9.00	49.50	49.51	49.50	
9.20	49.74	49.75	49.74	49.74
9.50	50.06	50.07	50.06	50.07
9.80	50.38	50.39	50.40	50.39
10.50	51.13	51.15	51.22	Limit of flat por-
11.00	51.66	51.69	51.84	tion of isother-
				mal correspond-
				ing to limit of
Cooling				$\left(\dfrac{\partial P}{\partial V}\right)_T = 0$ at
10.50	51.12	51.15	51.22	10.00°.
9.80		50.39	50.40	
9.50	50.06	50.07	50.06	
9.20	49.74	49.75	49.74	
9.00	49.50	49.51	49.50	

Discussion

The interpretation of these results is based on the assumption that the isothermals obtained by expansion from liquid densities are equilibrium curves and represent stable states of the system.   It is now realized that adequate proof of this is lacking.   However, the evidence obtained directly upon this point and published previously (2), together with all subsequent data, indicates that such is the case.

The experimental results show clearly that:

(1) Pressure isothermals above and below the temperature of meniscus disappearance contain regions of density wherein $\left(\dfrac{\partial P}{\partial V}\right)_T = 0$.   This region can no longer be observed on the isothermal at 10.00° C.

(2) The complete envelope of this region has been determined.

(3) The pressure of a heterogeneous system whose mean density is represented by a point within this envelope is the same as the pressure corresponding to the horizontal portion of the macroscopically homogeneous isothermal. The pressure of such heterogeneous systems is independent of the mass-volume ratio within such density limits.

(4) The pressure of heterogeneous systems corresponds exactly to the pressure of homogeneous systems obtained by heating at constant volume to 10.50° C. or higher, and cooling to the temperature at which the pressure of the heterogeneous system was measured, so long as the mean density of the system is within the envelope of the horizontal regions.

(5) A discrepancy between the value of the pressure at 9.50° C. obtained by Maass and Geddes (5) and that by the authors is apparent.   The pressure-

temperature curves of the former workers varied above 9.2° with mass-volume ratio. This result has not been duplicated. Indeed, the pressure-temperature values here given are independent of mass-volume ratio, provided that the mean density of the system lies within the region where $\left(\dfrac{\partial P}{\partial V}\right)_T = 0$.

(6) The pressure-temperature curves at constant volume are reversible.

Corroboration of Prediction by Mayer and Harrison

Harrison and Mayer, as already pointed out, have made calculations of particular interest as to the possible behaviour of a one component system in the critical-temperature–critical-pressure region (4). The theoretically predicted diagram given by these authors shows a startling similarity to that of the experimentally determined isothermals represented in Fig. 2. The continued existence of regions wherein $\left(\dfrac{\partial P}{\partial V}\right)_T = 0$ above the temperature of meniscus disappearance is completely verified by experiment. The suggested symmetry of this region about V_c is, however, not apparent. The experimental isotherms show a nearly perpendicular boundary for V_f, while V_s slopes noticeably toward the higher densities as the temperature is raised. V_s, V_f, and T_m have the same significance as in the nomenclature of Harrison and Mayer.

Explanation of Liquid Density Hysteresis Curve

From the above data it is apparent that a two phase system of liquid and vapour continues to exist above T_m, the temperature of meniscus disappearance. The two phases may or may not form an apparent homogeneous system, depending on the thermal treatment and mechanical stirring to which it has been subjected. The dispersion of one phase in the other is apparently possible because of a zero or very minute surface tension (9, 11). The value of the surface tension explains the equivalence of pressures of heterogeneous and homogeneous systems. With this hypothesis as the basis, a reasonable explanation for the density hysteresis of the liquid phase as measured by the spiral and float method may now be offered.

On heating a two phase system at constant volume from well below the critical temperature, the density of the liquid phase rapidly diminishes as the classical critical temperature is approached. A heterogeneous system continues to exist until the temperature is slightly above 10.00° C., where a homogeneous medium is formed. This system would be represented by a point somewhere above the shaded area of Fig. 2. It exhibits the behaviour of a one phase system. On cooling from this temperature, liquid re-forms and is distributed evenly throughout the tube, as the unchanging density value shows. As the temperature decreases, the interfacial tension between the phases increases, until at 9.20° C. it is sufficiently great for spontaneous stratification to occur, and a liquid phase is seen to separate. The apparent density of this liquid does not coincide with the liquid density on the original heating curve until a temperature of 8° C. has been reached (See Fig. 1).

This is believed to be caused by a residual quantity of vapour remaining suspended in the liquid. The amount of vapour that the liquid can retain decreases with decreasing temperature, until at 8° C. it is so small that the true liquid phase density is again exhibited. This concept has been incorporated in a previous paper to explain the effect of compression on the density and on the amount of the liquid that separates at 9.20° C. (9, 11). The fact that the phase densities at the classical critical temperature are a function of the mass-volume ratio (6) can also be explained by a mutual dispersion of the two phases. Further evidence supporting this hypothesis will be published shortly by Naldrett, Mason, and Maass (8).

Critical Constants as Determined from the Pressure-volume Isothermals

From the envelope of the region for which $\left(\dfrac{\partial P}{\partial V}\right)_T = 0$ the true critical constants of ethylene may be determined. The point of inflection, $\left(\dfrac{\partial^2 P}{\partial V^2}\right)_T = 0$, gives that temperature at which liquid can no longer exist under its own vapour pressure. The pressure, temperature, and specific volume of this point are respectively, 50.50 atm., 9.90° C., and 4.40 cc.

Vapour Pressure of Ethylene between 8.92° and 9.90° C.

The isothermals given above have been used to determine the vapour pressure curve of ethylene in the critical region. The values are given in Table III, and are represented in Fig. 3. The pressure for any one temper-
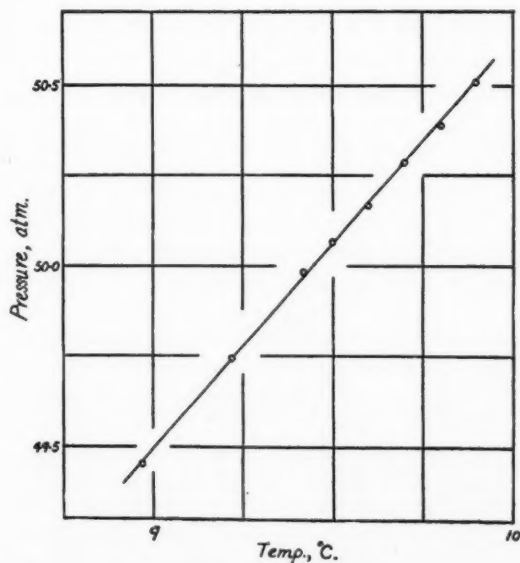

FIG. 3. *Relation between vapour pressure and temperature in the critical temperature region.*

TABLE III

VAPOUR PRESSURE OF ETHYLENE

Temp., °C.	8.92	9.22	9.42	9.50	9.60	9.70	9.80	9.90
Av. press., atm.	49.45_3	49.74_3	49.98_3	50.06_6	50.16_6	50.27_6	50.38_6	50.51_0

From Fig. 3. $\dfrac{\partial P}{\partial T} = \dfrac{50.600 - 49.450}{9.975 - 8.960}$ atm. /°C.

$$= \frac{1.150}{1.015} \text{ atm. /°C.} = 1.13_3 \text{ atm. /°C.}$$

ature was taken as the average of the pressures determined in the region for which $\left(\dfrac{\partial P}{\partial V}\right)_T = 0$. Although pressures are given in Table I to 0.01 atm. only, the average should be somewhat better, and the last figures in Table III have been included for this reason. As is to be expected over such a narrow range of temperature, the vapour pressure as a function of temperature is excellently represented by a straight line.

Heat of Vaporization in the Critical Region

The latent heat of vaporization may be calculated from the Clausius-Clapeyron equation,

$$T \frac{\alpha P}{\alpha T} = \frac{\lambda}{V_2 - V_1}$$

where λ is the latent heat of vaporization in cal. per gm.;

V_2 is the specific volume of the saturated vapour;

V_1 is the specific volume of the saturated liquid.

The value of $\dfrac{\alpha P}{\alpha T}$ was evaluated graphically from the figures of Table III, while the specific volumes of vapour and liquid were determined from the saturation curve of Fig. 2. These values are tabulated in Table IV, and the latent heat as a function of temperature is represented in Fig. 4. A latent heat is seen to exist at 9.50° C., which is the classical critical temperature.

TABLE IV

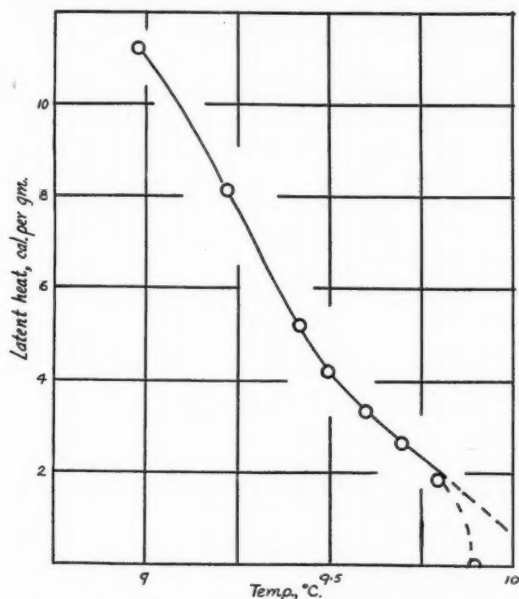| V_2	V_1	T	$\dfrac{\alpha P}{\alpha T}$	λ cal. /gm.	$V_2 - V_1$
5.448	4.000	282.1	1.13	11.19	1.448
5.176	4.072	282.4	1.13	8.53	1.104
4.896	4.224	282.6	1.13	5.20	.672
4.800	4.256	282.7	1.13	4.21	.544
4.688	4.256	282.8	1.13	3.34	.432
4.596	4.256	282.9	1.13	2.63	.340
4.520	4.280	283.0	1.13	1.86	.240
4.400	4.400	283.1	1.13	0	0

FIG. 4. *Relation between latent heat of vaporization and temperature in the critical temperature region.*

A better value of the temperature at which the point of inflection of the isothermals occurs may be obtained from an extrapolation of the latent-heat–temperature curve.   The temperature of 9.90° C. was taken since this is the last isothermal that exhibits a detectable region where $\left(\dfrac{\partial P}{\partial V}\right)_T = 0$. The sensitivity of the experimental method limits the accuracy of such a choice, and an improvement may be made by extrapolating the smooth curve of latent heat against temperature.   Such an extrapolation indicates a temperature of slightly more than 10.00° C., which is in excellent agreement with the temperature of minimum viscosity found by Mason and Maass (7).

Qualitative Description of Transition from Liquid to Gas

In addition to the evidence presented here, which suggests a dispersion basis for part of the process of transition, time lags have been recorded that are very great when a system in the "vapour" region of densities has its conditions changed in such a manner as to cause a shift toward "liquid" densities (5, 6, 8).   These time lags have been interpreted as indicative of a change in degree of orientation as the liquid state is approached.   From such data the following description of the changes that occur on liquefaction has been developed.   It is, in essence, a combination of the ideas proposed by Traube (8), Maass and his co-workers, and Bradley, Browne, and Hale (1).

The distinction made by Traube between real liquid (liquidons) and real gas (gasons), and between the liquid phase and the vapour phase might even even be retained subject to the following interpretations. In that case the liquid phase is to be considered as liquidons containing true gas in solution while the vapour phase contains true liquid in solution in gasons. The difference between a liquidon and a gason may be that a gason is a single molecular unit, or at least is made up of few molecules, whereas a liquidon is a group of gasons. On compression of a mass of gasons, orientation and clustering occur at random throughout the gas, and small groups of liquidons form and break up as the kinetic theory demands. Thus the life of any one group is limited, but such groups are always present. On further compression below the critical temperature the number of groups increases until saturation has been attained, and precipitation of the liquid phase occurs. This phase contains a saturation value of gasons. To quote directly from Bradley, Browne and Hale, "This view transforms the area of lique- faction on a diagram of isothermals to an area of saturation. Outside this area, on the side opposite the pressure axis, liquidons may exist, less or more according to volume, but never to the extent of saturating the gasons in which they are dissolved." With regard to gasons in the liquid the opposite is true. "Above the critical temperature, true gas and true liquid may exist side by side in any proportion, according to volume, but there can never be phases except in the loose sense of temporary stratification. Outside the area of saturation there is perfect continuity in every direction. The area of saturation, indeed, is after all only an exceptional case in an otherwise general continuity between the liquid and gaseous conditions of matter."

In the case of ethylene, below $9.20°$ C., the saturated phases of liquid and gas are separated into layers. Between this temperature and the tem- perature above which the molecular species are infinitely soluble one in the other ($10°$ C., approximately), two saturated phases co-exist, and remain in layers, or are dispersed one in the other, depending upon the treatment to which the system is subjected. Above this temperature a saturation value is impossible and the system acts as a one phase system. At sufficiently small densities it will exhibit the behaviour characteristic of a gas, and at very great densities it will exhibit that of a liquid.

A review will appear of the ideas held at present in this laboratory in regard to the nature of the change of state in the critical-pressure—critical-temperature region.

References

1. BRADLEY, W. P., BROWNE, A. W., and HALE, C. F.   Phys. Rev. 26 : 470-482.   1908.
2. DACEY, J., MCINTOSH, R. L., and MAASS, O.   Can. J. Research, B, 17 : 206-213.   1939.
3. DACEY, J., MCINTOSH, R. L., and MAASS, O.   Can. J. Research, B, 17 : 231-240.   1939.
4. HARRISON, S. F. and MAYER, J. E.   J. Chem. Phys. 6 : 87-100.   1938.
5. MAASS, O. and GEDDES, A. L.   Phil. Trans. Roy. Soc. A, 236 : 303-332.   1937.
6. MCINTOSH, R. L. and MAASS, O.   Can. J. Research, B, 16 : 289-302.   1938.
7. MASON, S. G.   Ph.D. Thesis.   McGill University.   1939.
8. NALDRETT, S. N., MASON, S. G., and MAASS, O.   Forthcoming publication.
9. PALL, D. B.   Ph.D. Thesis, McGill University.   1939.
10. TRAUBE, I.   Trans. Faraday Soc. 34 : 1234-1235.   1938.
11. WINKLER, C. A. and MAASS, O.   Can. J. Research, 9 : 65-79.   1933.

THE CONVERSION OF ALPHA-BROMONAPHTHALENE INTO THE BETA ISOMER[1]

By Herbert E. Fisher[2] and R. H. Clark[3]

Abstract

L. Roux found that α-bromonaphthalene was partly converted into β-bromonaphthalene by warming with aluminium chloride and carbon disulphide. Because of the interest in the β-derivatives for the preparation of naphthalene-2-acetic acid, one of the synthetic plant hormones, this investigation was undertaken to improve, if possible, upon the yield hitherto obtained. Several metals, notably antimony, molybdenum, nickel, and tungsten, in conjunction with aluminium chloride, gave increased yields.

Introduction

The conversion of α-bromonaphthalene into the more difficultly synthesized β-compound is of importance for the synthesis of naphthyl-2-acetic acid.

This transformation was first studied by Roux (2), who heated the α-compound with aluminium chloride in a carbon disulphide solution, and reported a yield of 15% of the β-derivative. He postulated the formation of an intermediate compound with aluminium chloride, which in turn decomposed, giving the β-isomer.

Mayer and Schiffner (1) found, by passing α-bromonaphthalene over silica gel in a porcelain tube at 350° C., that a very small quantity of the β-bromonaphthalene was formed. Attempts to make the β-bromo compound from β-naphthol directly have not been very successful (3).

Since any direct method for the preparation of β-bromonaphthalene did not appear to be promising, this investigation was undertaken to see whether the process originally developed by Roux could be modified to give an increased yield. Variations in temperature, solvents, and catalysts were employed.

Experimental

The reaction mixture was in every case placed in a 500 cc. Claisen flask, to one neck of which was attached a reflux condenser, to prevent loss of the volatile solvent; through the other neck passed a motor driven stirrer with a mercury seal. Local overheating was prevented by means of a second stirrer in the water bath.

Several attempts to follow the directions given by Roux gave a maximum yield of 9.1%, calculated on the basis of the α-bromonaphthalene utilized.

Among the modifications then employed was a change of solvent. The carbon disulphide was replaced by such solvents as acetone, benzene, aqueous and absolute alcohol, dioxane, aqueous and anhydrous pyridine, and nitromethane. No conversion whatsoever was obtained with these solvents.

Other catalysts, both to replace and to augment the action of the aluminium chloride, were then investigated. Freshly prepared anhydrous ferric chloride

was used in place of the aluminium chloride; no β-compound was obtained, the α-compound being recovered almost quantitatively.

Various multi-valent metals were then added in small quantities to the aluminium chloride, in search of a promoter for the reaction. A typical procedure was: 350 cc. of carbon disulphide, 100 gm. of α-bromonaphthalene, 10 gm. of anhydrous powdered aluminium chloride, and 0.5 gm. of nickel were placed in the Claisen flask, fitted with reflux condenser and mercury seal stirrer, and refluxed for one hour at 50° C. Preliminary experiments showed these to be the optimum conditions for the conversion. The contents of the flask were then decanted into cold water, stirred to dissolve any aluminium chloride, and the carbon disulphide layer was filtered to remove the nickel. The solvent was distilled off, after which the temperature was raised, and naphthalene, and a mixture of α- and β-bromonaphthalene, successively collected at temperatures of 220 to 260° C. and 270 to 310° C., respectively. The mixture was chilled to 5° C. in a refrigerator; the solid product was pressed between filter paper, while kept at this temperature, and the β-derivative collected, and recrystallized from 95% alcohol.

Table I gives the results obtained with various metals. The percentage yield is calculated on the basis of the α-bromonaphthalene utilized.

TABLE I

YIELDS OF β-BROMONAPHTHALENE WITH VARIOUS METALS

Promoter	β-bromo-naphthalene obtained, gm.	α-bromo-naphthalene recovered, gm.	Naphthalene, gm.	Yield, %
Antimony	18.0	20.0	10.5	22.5
Molybdenum	20.0	19.0	13.0	25.0
Selenium	13.0	21.0	11.8	16.0
Nickel	22.0	14.0	14.5	25.5
Tungsten	18.0	13.5	15.0	23.5
Chromium	12.5	13.5	11.5	14.4
No promoter	8.5	7.0	10.5	9.1

Remarks

Carbon disulphide would appear to be the only solvent suitable for the conversion of α-bromonaphthalene into the β-bromonaphthalene. Although it was found that a practically quantitative recovery of the solvent was possible at the end of the heating period, it is not improbable that an intermediate compound is formed with the carbon disulphide.

The mechanism of the action of promoters is still obscure. Since several reactions are taking place simultaneously, such as the production of naphthalene, β-bromonaphthalene, dibromonaphthalene, hexabromonaphthalene, and tar, it is possible that the promoter retards the side reactions, or accelerates the main reaction.

References

1. MAYER, F. and SCHIFFNER, R.   Ber. 67, B : 67-69.   1934.
2. ROUX, L.   Ann. chim. phys., 12 : 6.   1887.
3. SONTAG, D.   Ann. chim., 11 : 354-438.   1934.

STARCH CONTENT OF CERTAIN WHEATS OF THE 1935 CROP[1]

By Clarence Yardley Hopkins[2]

Abstract

Average samples of 12 grades of Western Canadian wheat (1935 crop) were analyzed for starch by a polarimetric method. The samples of the ordinary milling grades, in which Marquis was the predominant variety, contained from 50 to 52% of starch on a basis of 13.5% moisture. Samples of Garnet wheat contained about 55% starch. Rusted wheat had a lower starch content. There is positive correlation between starch content and specific gravity of the kernels.

Comparison with data obtained elsewhere on the same samples shows that the sum of the starch and protein is closely related to the flour yield.

Introduction

In connection with a survey of possible industrial uses for Canadian wheat, the starch content of a number of samples of the 1933 crop was determined (4). In that year the grain was of high quality and a very large percentage was graded One and Two Northern.

The 1935 crop was more widely distributed among the various grades. Three special grades were also set up to provide for seriously rusted wheat and two new grades were established for Garnet wheat. Representative samples were therefore obtained from 12 different classifications including the rusted grain and the Garnet variety.

The samples were supplied through the kindness of Dr. W. F. Geddes of the Grain Research Laboratory at Winnipeg. They were taken from the "Winnipeg Averages", which are composite samples representative of the wheat passing through Winnipeg to eastern markets.

Experimental

The grain was cleaned, ground, and analyzed for moisture in accordance with the methods described previously (4). Starch determinations were made by a polarimetric method (3). The analytical results are given in Table I.

The specific gravity of the kernels was determined by the pycnometer method of Bailey and Thomas (1).

A graphical comparison of starch content, specific gravity, and weight per bushel is shown in Fig. 1. The figures for weight per bushel are taken from the annual report of the Grain Research Laboratory (2), as are the data on protein content and flour yield shown in Fig. 2. The determinations were made on the same composite samples that were used in the present investigation.

The correlation between starch content and specific gravity is high ($r =$ .86; 1% point $= .71$).

TABLE I

STARCH CONTENT OF WHEAT SAMPLES FROM 1935 CROP

| Grade of wheat	Moisture, %	Starch, % (as received)		Starch, % (13.5% moisture basis)
1 Hard	8.40	(55.22, 55.39)	55.31	52.23
1 Northern	8.62	(53.55, 53.65)	53.60	50.74
2 Northern	9.57	(54.00, 53.89)	53.95	51.60
3 Northern	8.44	(53.84, 53.91)	53.88	50.90
4 Northern	8.21	(53.09, 53.23)	53.16	50.09
5 Wheat	8.35	(53.25, 53.35)	53.30	50.30
6 Wheat	7.83	(52.02, 52.28)	52.15	48.94
4 Special	7.82	(52.53, 52 66)	52.60	49.35
5 Special	7.26	(51.37, 51.47)	51.42	47.96
6 Special	6.87	(51.45, 51.47)	51.46	47.80
1 C.W. Garnet	7.36	(58.91, 59.21)	59.06	55.14
2 C.W. Garnet	8.05	(58.13, 58.22)	58.18	54.74
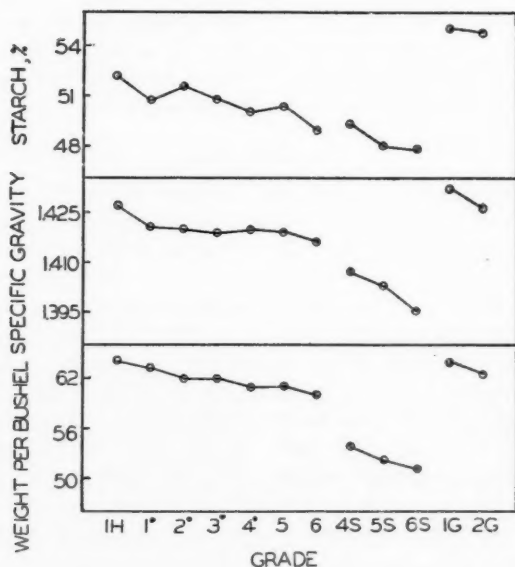
FIG. 1. *Comparison of starch content of wheat with physical properties of the kernels.*

Starch Content and Flour Yield

A comparison of starch content, protein content (2), and flour yield (2) is shown graphically in Fig. 2. Both starch and protein content decline irregularly from the higher to the lower grades. The Garnet samples are characterized by low protein and high starch content.
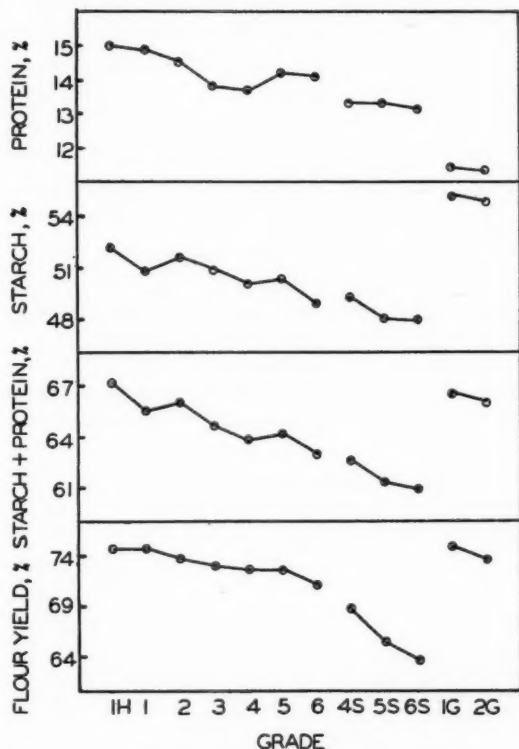

FIG. 2. *Comparison of starch content, protein content, and flour yield of wheat.*

There is a very close relation between the flour yield and the sum of the starch content and protein content in these samples. The relation, however is curved and is given by the equation

$$y = -1269.69 + 40.2504x - .301309x^2.$$

where y = flour yield and x = starch content + protein content (Fig. 3).

This equation fits the data almost exactly, the multiple correlation being $R = .986$. The result of these analyses indicates that it may be possible to predict the flour yield of new varieties of wheat by determining starch and protein content, using a relatively small sample.
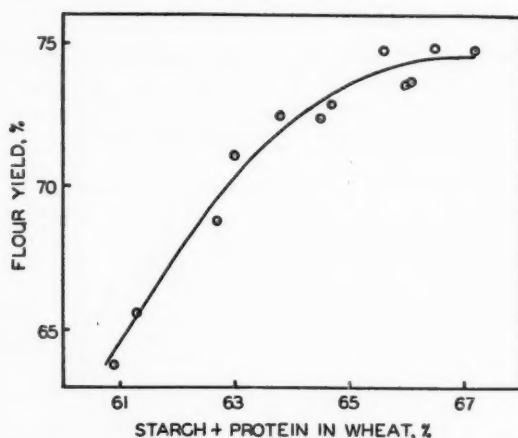
Fig. 3. *Relation between flour yield and starch + protein. The experimental results are plotted along with the curve which represents the mathematical relation between these two variables.*

The protein content of the Garnet grades seems to be unusually low in these crop samples.   However, the sum of the starch and protein is practically the same as in the corresponding grades of Marquis wheat (Table II).

TABLE II
MARQUIS AND GARNET SAMPLES
(13.5% moisture basis)

Grade	Starch, %	Protein, % (2)	Starch + protein, %
1 Northern (Marquis)	50.7	14.9	65.6
2 Northern (Marquis)	51.6	14.5	66.1
1 C.W. Garnet	55.1	11.4	66.5
2 C.W. Garnet	54.7	11.3	66.0

TABLE III
COMPARISON OF SAMPLES FROM 1933 AND 1935 CROPS
(13.5% moisture basis)

Grade	Starch, %		Protein, %		Starch + protein, %	
	1933	1935	1933	1935 (2)	1933	1935
1 Northern	51.9	50.7	14.4	14.9	66.3	65.6
2 Northern	52.0	51.6	14.0	14.5	66.0	66.1
3 Northern	50.1	50.9	14.5	13.8	64.6	64.7
4 Northern	51.0	50.1	13.2	13.7	64.3	63.8
5 Wheat	52.0	50.3	12.2	14.2	64.2	64.5
6 Wheat	51.5	48.9	12.8	14.1	64.3	63.0
Mean	51.4	50.4	13.5	14.2	64.9	64.6

Comparison with 1933 Crop Analyses

The previous investigation (4) included analyses of some samples of the 1933 crop from the grades 1 Northern to 6 inclusive. Comparative figures are shown in Table III.

The starch content of the 1935 crop samples is somewhat lower and the protein content somewhat higher than was found in the 1933 samples. The sum of the starch and protein, however, is virtually the same.

The three special grades of the 1935 crop, containing heavily rusted wheat, were shown to be low in protein (2). It had been expected that these grades, made up in large proportion of shrunken kernels, would be low in starch but high in protein owing to the high ratio of bran and germ to endosperm.

Since both starch and protein are lower than in undamaged wheat, it is concluded that the content of fibre and hemicelluloses must be correspondingly higher.

References

1. BAILEY, C. H. and THOMAS, L. M. U.S. Bur. Plant Ind. Circ. No. 99. 1912.
2. DOMINION GRAIN RESEARCH LABORATORY (Canada). 9th Ann. Rept. 1935.
3. HOPKINS, C. Y. Can. J. Research, 11 : 751-758. 1934.
4. HOPKINS, C. Y. and GRAHAM, R. P. Can. J. Research, 12 : 820-824. 1935.

2 : 2'-BIQUINOLYL—A REAGENT FOR COPPER[1]

By J. G. Breckenridge,[2] R. W. J. Lewis,[3] and L. A. Quick[3]
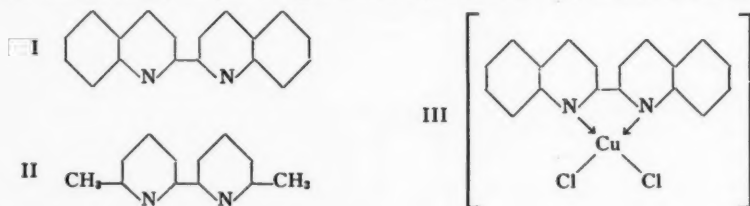
Abstract

2 : 2'-Biquinolyl, prepared by catalytic dehydrogenation of quinoline, has been found to give a purple colour with the cuprous ion under certain conditions. The colour reaction is sensitive, specific for copper, and the intensity of the colour produced follows Beer's law. A procedure has been worked out for the detection and estimation of copper, the smallest amount of copper detectable being 1 part in 100,000,000. Stable complexes with cupric copper and cobalt have also been prepared.

Introduction

Co-ordination compounds of 2 : 2'-bipyridyl with many metals are well known, such as that with ferrous iron, which has become widely used as the basis for the colorimetric estimation of iron. 2 : 2'-biquinolyl (I), although of similar character, has been little investigated, an exception being the work of Smirnoff (4), who showed that it fails to give a colour reaction with ferrous iron. He considered the reason for this to lie in the difference between the ring structures of quinoline and pyridine, that of quinoline being supposed to be analogous to the structure for naphthalene proposed by Willstatter (7). In the light of more recent theories as to the structure of the naphthalene and quinoline rings (3), Smirnoff's hypothesis would seem to be faulty, and, in any case, to draw conclusions about the structure of the heterocyclic rings from one negative observation seemed to the writers to be unwarranted. Willink and Wibaut (6) found that 6 : 6'-dimethyl-2 : 2'-bipyridyl (II) also gave no reaction with ferrous iron, and it was felt that the behaviour of biquinolyl with metals other than iron should be investigated.

Results and Discussion

It has been found that biquinolyl gives stable compounds with cupric and cobaltous salts, and also forms a purple complex in solution with cuprous copper. The compounds formed with cupric and cobaltous chloride are of the type (Biq .MX$_2$), and it is probably that, in view of their insolubility in water and alcohol, they are represented by Formula III, the chlorine atoms

being held within the complex by covalent links. The compound formed from ethylenediamine and cupric chloride has been shown by Chattaway and Drew (1) to exist as the dimeric form $(Cu\ en_2)CuCl_4$, and it is possible, though unlikely, that the $CuCl_2$-biquinolyl compound is of similar character.

The $CuCl_2$-biquinolyl compound is orange coloured and is precipitated when solutions of the base in hydrochloric acid, acetic acid, or alcohol are mixed with a solution of the cupric salt. Changing the proportions of the reagents did not affect the character of the product, even a large excess of the base and prolonged heating making no difference. The compound prepared from copper sulphate and the base is light green and crystalline.

The $CoCl_2$-biquinolyl compound is light green, and is best prepared by mixing alcohol solutions of the reactants. As with copper, no other form could be obtained. No reaction was observed between the base and cobaltic hexamminochloride in dilute alcohol, even on prolonged heating.

The complex formed with cuprous copper is deep purple in solution, and is obtained when solutions of a cuprous salt in dilute hydrochloric acid, acetic acid, alcohol, or dioxan are mixed with solutions of the base. The tendency to form the purple complex is very strong, as the colour is produced when metallic copper comes in contact with an alcohol solution of the base, and also when the cupric compounds described above stand in contact with alcohol for some time. The colour is not noticeably affected by exposure to sunlight over a long period, by boiling for several hours, or by bubbling air through the solution for several days.

These results indicated that biquinolyl might be of value as a reagent for the colorimetric estimation of copper, and tests were carried out to determine the optimum conditions for development of the colour. In the preliminary work a standard copper sulphate solution was made up, containing 5×10^{-5} gm. copper per ml., and to known volumes of this were added 4 drops of sodium sulphite solution (500 gm. in one litre of water) 2 ml. of ethanol, 14 drops of a solution of biquinolyl in ethanol (0.5 gm. in 100 ml.), and the volume was made up to 6 ml. with water. The resulting solutions were observed in a Klett colorimeter, and the values obtained showed that the colour intensity obeyed Beer's law, within the limits of error of the method employed.

The following ions were tested in dilute hydrochloric acid or ethanol solution, and were found to give no colour reaction with the base:— Na^+, K^+, Li^+, Be^{++}, Mg^{++}, Ca^{++}, Ba^{++}, Zn^{++}, Cd^{++}, Hg^+, Hg^{++}, Al^{+++}, Sn^{++}, Sn^{++++}, Pb^{++}, Sb^{+++}, Bi^{+++}, Fe^{++}, Fe^{+++}, Co^{++}, Ni^{++}, Mn^{++}, Ag^+, Ce^{++++}, Zr^{++++}, Cs^+, Cr^{++}, and Sr^{++}. Titanium trichloride gave a pale green colour with an ethanol solution of the base. The colour reaction was apparently therefore specific for cuprous copper, and further work was done to determine more precisely the relation between the colour intensity and the amount of copper present.

Experimental

The instruments used were a Pulfrich Gradation Photometer and an Evelyn photoelectric colorimeter (2). To determine the proper filter for use in these

instruments, the colour absorption curve of a solution containing 4×10^{-5} gm. of copper in 50 ml. was plotted; the result is shown in Fig. 1.   Since the percentage transmission was lowest at about 530 mμ, the filter selected for use with the Pulfrich Photometer was the L_2, which has a transmission maximum at this wave-length.   In work with the photoelectric colorimeter, a filter having a maximum at 540 mμ was employed.
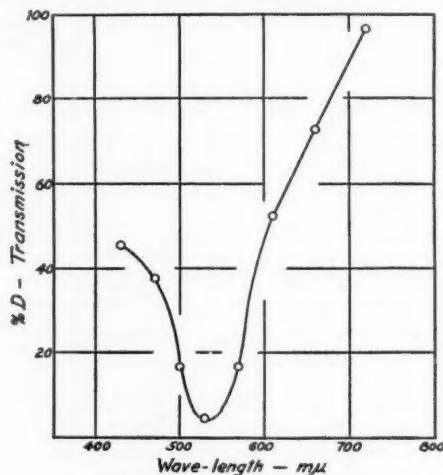

FIG. 1.   *Colour absorption curve.*

The procedure finally adopted in making up the solutions for measurement was as follows—varying amounts of a standard copper solution (4×10^{-5} gm. copper per ml.) were taken, using standardized Exax Ostwald pipettes.   To the copper sample was added 5 ml. of sodium bisulphite solution (10 gm. in 100 ml. water), 1 ml. of a solution of biquinolyl in glacial acetic acid (0.5 gm. per litre), and the solution made up to 50 ml. with glacial acetic acid.   The pH of the resulting solution was found to be between 1.55 and 1.75.   A series of results obtained using the photoelectric colorimeter, with samples containing from 0.2×10^{-4} to 2.4×10^{-4} gm. of copper are shown in Figs. 2 and 3, and it is evident that the colour intensity obeys Beer's law.   Since the percentage transmission, G, could be read only to within 0.25% on the galvanometer scale, the limits of accuracy were $\pm 1\%$ of the amount of copper present.   The lower limit for accurate readings was found to be with a solution containing 4×10^{-7} gm. of copper, while the lowest amount of copper necessary to give a perceptible deflection on the galvanometer was 8×10^{-9} gm., or approximately 1 part in 100,000,000.   A solution containing 1 part of copper in 10,000,000 could easily be distinguished from a blank, using a 7 cm. depth of solution in a Klett colorimeter.   The blank solutions for the photoelectric colorimeter, if exposed to sunlight for several days, showed a decrease in transmission of approximately 0.5%, and they were therefore made up freshly for each series of determinations.

When the general method indicated above had been worked out, tests were performed to investigate interference by other metals.   It was found that the method was accurate with sodium, potassium, or magnesium present in $1000x$ the amount of copper; manganese or phosphate, $50x$; and nickel, $10x$.   If more nickel was present it had to be removed with dimethyl-glyoxime, an excess of this reagent not interfering with the subsequent determination of copper.

Iron, although it gives no perceptible colour with biquinolyl, nevertheless interfered by reducing the percentage transmission, thus giving a high value for the copper.   When the same amounts of iron and copper were present, the percentage transmission was about 1% lower than with copper alone. Any iron present in a sample was therefore precipitated in the usual manner
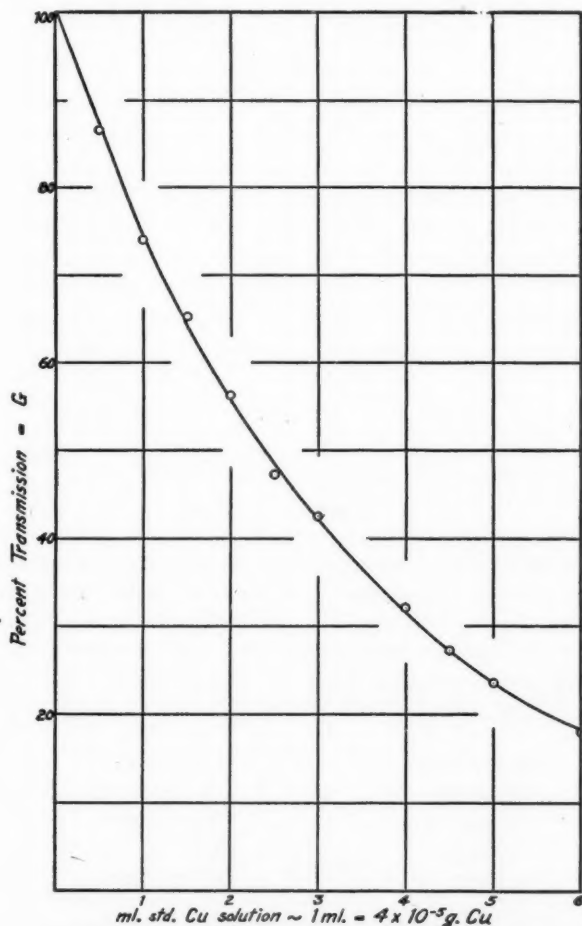

FIG. 2.   Calibration curve using photoelectric colorimeter.

with bromine water and ammonia, the precipitate redissolved and reprecipitated, and the copper determined in the acidified filtrate in the normal manner.
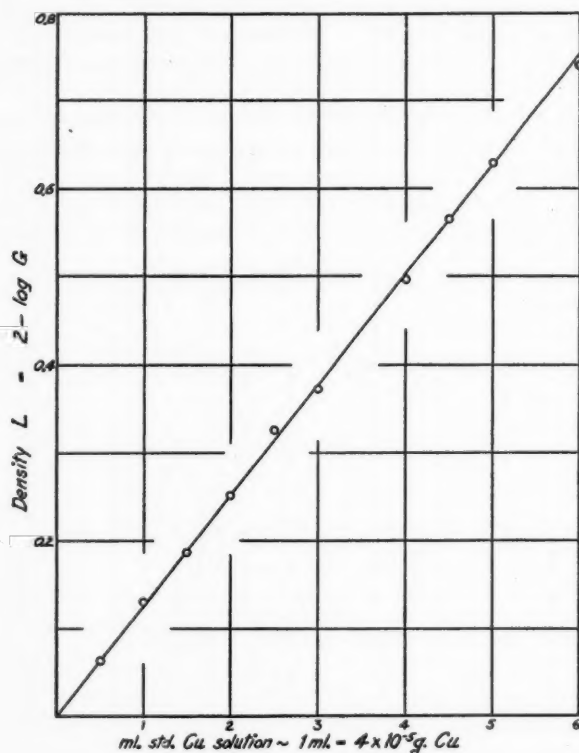

FIG. 3.   *Application of Beer's law.*

It was thought desirable to check this method for copper against the ordinary electrolytic determination.   A sample of nickel ore was obtained containing approximately 2% of nickel and 0.9% of copper, with some iron present.   After the iron had been removed as described above (but not the nickel), samples were analyzed by the colorimetric method, and by an independent analyst using the standard electrolytic method, with the following results—

	Colorimetric	Electrolytic
	0.902%	0.892%
	0.906	0.890
	0.942	0.910
	0.905	0.930
Av.	0.91% copper	0.90% copper

It was found impossible to isolate in a pure state the complex responsible for the purple colour. Early experiments on the change of colour intensity with varying amounts of biquinolyl showed that there must be at least two molecules of the base present for every Cu atom, and analysis of an evidently impure product confirmed this ratio. The probable structure of the ion which is responsible for the colour is IV. The anion present in the solution does not affect the colour in any way, as far as could be found.

IV
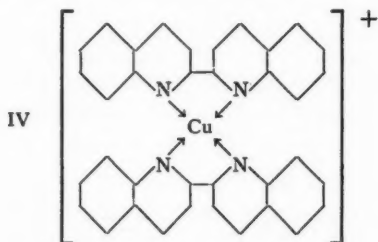
The method described above for the determination of copper, and also for its detection when present in small amounts, would seem to be accurate and comparatively simple to use, but is handicapped by the unavailability of the reagent. As noted later, an increased yield is possible by use of the original catalytic method of Wibaut, Willink, and Nieuwenhuis (5), and it is intended to investigate this further.

The precipitate obtained with cupric salts in acid solution may also prove to be of use as a gravimetric precipitant for copper, and this point is also under investigation.

Preparation of Biquinolyl

This was prepared according to the method of catalytic dehydrogenation of quinoline given by Wibaut *et al.* (5), the nickel-alumina catalyst being prepared according to the method of Zelinsky and Kammarewsky (8). The yields obtained by the former were about 15%. It was found, however, that by following the procedure indicated below, the yield could be raised to nearly 50%. The apparatus shown in Fig. 4 was used, the catalyst being
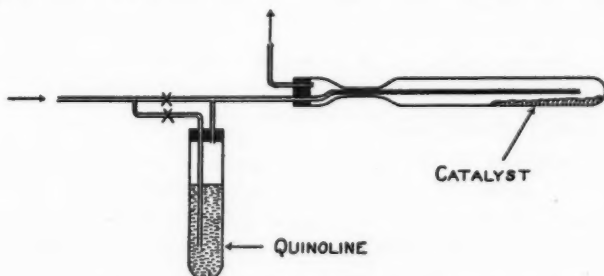

CATALYST

QUINOLINE

FIG. 4. *Apparatus used in preparation of biquinolyl*

reduced in the Carius tube at 325° C. for 20 hr. The tube was then swept out with nitrogen, the flask containing the quinoline inverted, and the quinoline forced into the tube, which was then sealed, and heated as described by Wibaut *et al.* (5). A typical run gave the following results—9 gm. of catalyst (weight before reduction) with 45 gm. of quinoline heated to 330° C. for eight hours gave 9.9 gm. of biquinolyl (m.p. 195 to 196° C.*) and a recovery of 25 gm. quinoline, or a yield of 48%. Six runs of this size averaged a yield of 45%. The contents of the Carius tubes after cooling was almost solid with crystals of the product, very little or no tar being formed. (It should be mentioned that in some early work on this synthesis, a student developed a short-lived skin rash, apparently due to handling the tar.) The quinoline used was a synthetic product, and was dehydrated and twice distilled before use.

Compound with Cupric Chloride

This was prepared by mixing solutions of the base and cupric chloride in dilute hydrochloric acid, 50% acetic acid, or ethanol. The product from ethanol was microcrystalline, from the other solvents, amorphous, and possessed a bright orange-red colour. It was insoluble in hot acid solution, water, ethanol, and benzene, and was decomposed by alkaline solutions or by boiling with water. On standing in contact with ethanol the water solution gradually assumed the purple colour characteristic of the cuprous complex. It melted sharply at 338° C. with decomposition. Analysis gave the following results. Calcd. for $C_{18}H_{12}N_2 \cdot CuCl_2$: C, 55.32; H, 3.10; N, 7.17; Cl, 18.14%. Found†: C, 55.42, 55.36; H, 3.14; 3.22; N, 7.13; Cl, 18.85, 18.65%.

Compound with Copper Sulphate

Methanol solutions of the reactants when mixed gave small green crystals of the product. This was not investigated further, except that it was observed that on the addition of hydrochloric acid the orange colour, characteristic of the cupric chloride compound, appeared.

Compound with Cobaltous Chloride

This could be obtained either from ethanol or dilute acetic acid solutions of the reactants, the product from ethanol crystallizing as shiny grass-green leaves. It was similar to the cupric chloride compound in its behaviour. It had a melting point higher than 360° C. Calcd. for $C_{18}H_{12}N_2 \cdot CoCl_2$: C, 55.98; H, 3.13; N, 7.28; Cl, 18.36%. Found†: C, 56.00, 56.24; H, 3.13, 3.21; N, 7.35, 7.39; Cl, 18.42, 18.24%.

Compound with Cuprous Chloride

This was isolated by mixing the reactants in anhydrous ethanol in the proportion of 2 moles of base to 1 mole of cuprous chloride. The deep purple solution was evaporated, and the residue redissolved in ethanol, filtered, and again evaporated. This procedure was repeated six times, the final product

---

* *Melting points are corrected.*
† *Microanalyses by Miss J. Romeyn, Department of Chemistry.*

being a brownish-green microcrystalline solid.   It was much more soluble in ethanol than either reactant, and was insoluble in water or benzene.   It decomposed gradually on heating above 195° C.   Analysis gave the following results†:   C, 73.75; 73.35; H, 4.25, 4.13; Cl, 5.04, 4.92%.   Calcd. for $(C_{18}H_{12}N_2)_2$. CuCl: C, 70.8; H, 3.93; Cl, 5.8%.   Calcd. for above formula with 20% of biquinolyl present as impurity: C, 73.5; H, 4.1, Cl, 4.7%.

Acknowledgments

† *Microanalyses by Miss J. Romeyn, Department of Chemistry.*

References

1. CHATTAWAY, F. W. and DREW, H. D. K.   J. Chem. Soc. 947-948.   1937.

2. EVELYN, K. A.   J. Biol. Chem. 115 : 63-75.   1936.

3. GILMAN, H.   Organic chemistry.   John Wiley and Sons, New York.   1938.

4. SMIRNOFF, A. P.   Helv. Chim. Acta, 4 : 802-811.   1921.

5. WIBAUT, J. P., WILLINK, H. D. T., and NIEUWENHUIS, W. E.   Rec. trav. chim. 54 : 804-807.   1935.

6. WILLINK, H. D. T. and WIBAUT, J. P.   Rec. trav. chim. 54 : 275-283.   1935.

7. WILLSTÄTTER, R. and WASER, E.   Ber. 44 : 3423-3445.   1911.

8. ZELINSKY, N. and KAMMAREWSKY, W.   Ber. 57, B : 667-669.   1924.

THE TIME OF SET OF SILICA GELS

III. THE CHANGING EFFECT OF ALCOHOLS OVER A pH RANGE[1]

BY L. A. MUNRO[2] AND J. A. PEARCE[3]

Abstract

The effect of alcohols on the setting time of silica gels has been studied through a pH range. .

The total effect and the divergence of the individual behaviour of both monohydric and polyhydric alcohols become greater as the alkalinity of the gel is increased. When the time of set with addition agent is plotted as percentage of the original time of set, there is a constant effect for an equal number of alcohol molecules at pH 7. This apparently eliminates the dielectric constant of the alcohol as a decisive factor in coagulation. When the system is acidic, all the alcohols behave as retarders; when it is alkaline, only the higher polyhydrics act in this manner. The monohydrics and glycol change from accelerators to retarders at pH values between 7.4 to 8.5. The pH at reversal for each addition agent does not coincide with the pH at which the original gel shows minimum setting time.

Introduction

Hurd and Carver (7) have shown that the addition of ethyl alcohol increased the time of set of acid silica gels, whereas glycerol had a negligible effect. The pH of the gel was unaltered. Prasad and Hattiangadi (13) observed that the effect of methyl, ethyl, and propyl alcohols on alkaline gels was opposite to that on acid gels.

Munro and Alves (9) extended the series and found a regular decrease in the time of set of alkaline silica gels with increasing molecular weight of the monohydric alcohols. They observed that gels of high pH become more alkaline on setting, and that the effect seemed to be increased in the presence of the addition agents. It was also observed that though glycol decreased the time of set of these gels, its effect was not nearly so great as that of the monohydric alcohols. With glycerol the time of set was lengthened, i.e., the effect was similar to that brought about by addition agents in acid gels. The observations of Hurd and Carver on the effect of glycerol on acid gels were reinvestigated and their findings confirmed.

Munro and Pearce (12) found that the effect of glycerol was merely a part of a further and regular increase in the time of set when higher polyhydric alcohols were added to alkaline gels. It was also noted that, in the neighbourhood of pH 8.2, glycol changed from an accelerator of gelation to a retarder.

It was accordingly thought desirable to determine whether other alcohols show a reversal of their effect with changing pH; and further, whether this shift in behaviour has any relation to the pH at which the original gel shows minimum setting time.

Previous results suggest that the pH at reversal will vary with the addition agent. If the pH at inflection varies, it would be of interest to ascertain whether the monohydric and polyhydric alcohols behave as groups.

Experimental

Baker's best grade of "crystalline sodium silicate $Na_2SiO_3.9H_2O$" was used (12). Analysis showed a molar ratio of $Na_2O : SiO_2 = 1.00 : 1.02$. The water used for making up solutions was redistilled and boiled before use. A stock sodium silicate solution of specific gravity 1.1569 (Westphal balance) and containing 6.7% SiO_2 by analysis was used. From this stock supply, solutions of various strengths were made as required.

After work had been started it was observed that the '3.35% SiO_2' silicate solution gave a gel setting too fast to permit an accurate study through the region of minimum time of set. A sodium silicate solution of specific gravity 1.0500 containing 2.51% SiO_2 by analysis was therefore prepared.

The silicate solutions were kept in stoppered, waxed, Pyrex flasks.

The acid was prepared, as before, by diluting glacial acetic with 500 cc. of water; this yielded a 1.636 N solution. The addition agents were Eastman's best grade supplemented by sorbitol from Schuchardt.

The procedure of mixing, temperature control, and determination of the time of set was the same as that followed previously (12). The rise in temperature on mixing was constant, except for pH values greater than 9.0. The temperature of the mixing thermostat was adjusted for the required change. It might be emphasized here that to prevent esterfication the alcohol and acid were kept separate until the moment of mixing.

The pH values were determined with the Coleman glass electrode.

Results

The results are given in Table I. The times of set given are the mean values of two to six determinations. The accuracy obtainable decreases with the dilution of the gel and with the increased time of set. The average deviation is $\pm$ 5%.

There was an increase of pH on setting which continued for some time afterwards. The increase is not great in the case of the acid gels: e.g., original pH, 6.0; pH on setting, 6.1; with a final value of 6.1 after 24 hr. With alkaline gels the increase is as much as 0.4 pH units, e.g., 9.4 to 9.6 to 9.8.

With the polyhydric alcohols the initial and final pH values of the gel were not essentially different from those of the original. The monohydric alcohols, however, with alkaline gels, gave an increase of 0.1 to 0.2 pH units, the effect being in the order: n-propyl, ethyl, methyl. The effect with neutral and acid gels was very slight.

Fig. 1 shows the curves for the effect of different addition agents on the set of the gels prepared with the '2.23% SiO_2' silicate solution, at pH 7.8. (The notation for all the curves is shown in Fig. 2.) It will be observed that

TABLE I

EFFECT OF ALCOHOLS ON THE TIME OF SET OF SILICA GELS DIFFERING IN CONCENTRATION AND pH

Molar conc. of alcohol	Silicate solution used								
	'2.5% SiO₂'						'2.23% SiO₂'	'3.35% SiO₂'	
	Initial pH								
	9.4	8.5	7.4	6.6	6.1	5.6	7.8	7.4	6.0
	Min.	Min.	Min.	Min.	Min.	Min.	Sec.	Sec.	Min.
0.00	14.0	8.5	11.3	41.0	119	310	540	210	60.0
Methanol									
0.50	11.3	7.6	11.7	43.5	125	324	545	224	63.0
0.99	9.2	7.2	11.8	45.0	129	336	552	230	65.5
1.49	7.3	6.8	11.9	46.5	133	351	552	245	69.0
Ethanol									
0.34	10.1	7.7	11.3	43.8	132	333	–	–	64.0
0.69	7.0	6.5	11.3	46.0	138	360	–	–	68.5
1.03	5.0	5.5	11.2	48.3	144	382	–	–	72.0
n- Propanol									
0.27	9.0	7.3	11.1	44.5	135	340	–	–	66.0
0.54	5.6	6.3	11.1	47.8	147	373	–	–	73.0
0.80	3.3	5.2	11.0	50.0	154	403	–	–	79.0
Glycol									
0.36	13.0	8.6	11.8	42.8	124	322	570	216 ·	63.0
0.72	12.0	8.6	12.2	44.3	127	333	585	225	65.0
1.07	11.3	8.6	12.3	45.5	130	344	595	230	67.0
Glycerol									
0.27	15.4	8.9	11.7	42.0	122	315	570	216	61.0
0.55	16.0	9.3	12.0	42.5	124	319	585	220	62.0
0.82	16.5	9.5	12.2	43.5	126	326	600	225	63.0
Erythritol									
0.16	15.7	9.0	11.5	41.5	121	314	570	216	61.0
0.33	16.8	9.5	11.9	42.0	122	316	585	220	61.3
0.49	18.0	10.0	12.3	42.5	123	318	600	225	62.0
Mannitol									
0.11	17.5	9.3	11.8	41.5	119	313	510	216	60.5
0.22	18.9	9.8	12.0	41.8	120	314	600	220	60.8
0.33	20.0	10.5	12.3	42.0	121	315	615	225	61.0
Sorbitol									
0.11	16.6	–	11.8	–	–	–	–	–	–
0.22	18.2	–	12.0	–	–	–	–	–	–
0.33	19.5	–	12.5	–	120	–	–	–	60.3

not only is glycol a retarder, as indicated by the previous work, but, that at this pH, methyl alcohol has, in its effect, also changed from an accelerator to a retarder. Further, the retarding action of the others is practically unchanged [compare (12, Fig. 4)].
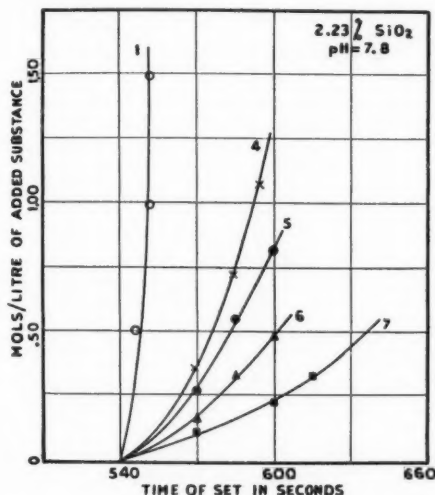

FIG. 1. *Silica gels, initial pH 7.8, prepared from 25 cc. of sodium silicate solution containing 2.23% SiO$_2$ + 25 cc. of acid mixture (12.7 cc. of acid + addition agent + water).*

With the gels from '3.35% SiO$_2$' silicate solution at pH 7.4 a similar shift in effect is noted (Fig. 2), both methyl alcohol and glycol now lengthening the time of set. With this gel concentration, the effect of methanol and glycol is reversed somewhere between pH of 7.4 and 8.8. The retarding action of the others is diminished, and the specific nature of the effect is less.

In order to eliminate any effect of gel concentration it was decided to make a series of measurements on gels of one standard silicate solution at a series of pH values.

The setting times for gels of each concentration of silicate and standard acid can be determined only over a limited pH range. This range is represented by the steep portion of the titration curves. Beyond this a large variation in the amount of standard acid causes a negligible change in pH, although a variation of even a fraction of a drop of the acid will change the time of set appreciably. The addition of stronger acid will extend the steep portion of the curve to lower pH values, but it results in gels having much longer times of set, with increase in the difficulty of determining accurate values (cf. Fig. 12).

A '2.5% SiO$_2$' silicate solution was chosen, as it gave convenient times of set. The titration curves for this solution and 1.636 N acid are shown in
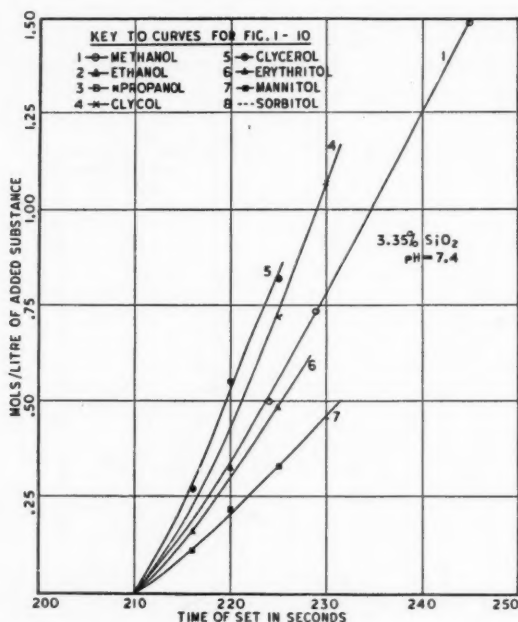
FIG. 2.　*Silica gels, initial pH 7.4; 25 cc. of sodium silicate solution (3.35% SiO_2) + 25 cc. of acid mixture (19.0 cc. of acid + addition agent + water).*

Fig. 3.　Here the pH is plotted against standard acid added for a constant amount of silicate solution (25 cc.), the total volume being kept constant (50 cc.). Curve I is for a fresh silicate solution, and Curve 2 for a silicate solution six months old. The latter gives slightly longer times of set (12). The shift may be due to the absorption of carbon dioxide, in spite of the precautions taken, or to colloidal changes in the 'sodium silicate'.
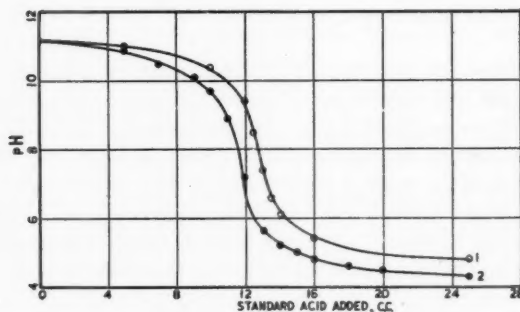

FIG. 3.　*Titration curves for silicate solutions containing 2.5% SiO_2 versus the standard acetic acid. Curve 1, fresh, Curve 2, aged, silicate.*

The results with gels from the '2.5% SiO₂' silicate solution for this range of pH values are shown in Figs. 4 to 9.

It will be noted that the curves are widely divergent at pH 9.4 (Fig. 4), although the order of the effect in each case is the same as that noted in previous studies, viz., *n*-propyl, ethyl, methyl, glycol, glycerol (9), followed by erythritol and mannitol (12). The values obtained with sorbitol are not very different from those observed with its isomer, mannitol.
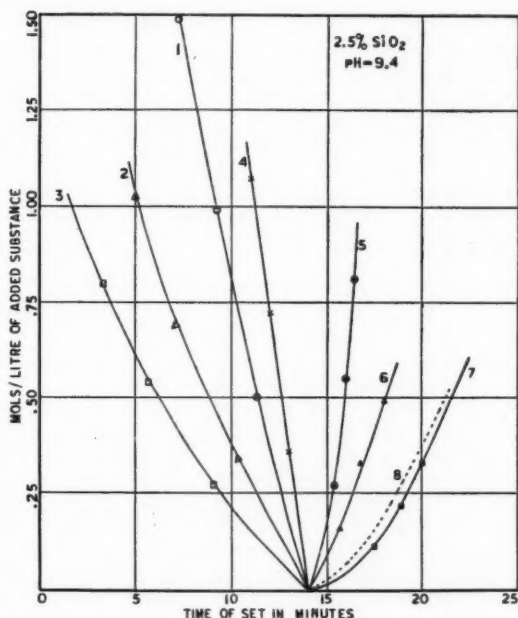

FIG. 4. *Silica gels, initial pH 9.4; 25 cc. of sodium silicate solution (2.5% SiO₂) + 25 cc. of acid mixture (13 cc. of acid + addition agent + water).*

The values for pH 8.5 are shown in Fig. 5. At this hydrogen ion concentration, glycol produces only a very slight change in the time of set. The order of the other curves is the same, but the effects are less pronounced, i.e., the curves have moved toward a zero effect. This diminution in specificity is more noticeable at pH 7.4, as will be seen in Fig. 6. Here, however, it is observed that methanol has become a retarder, and that now ethanol has a zero effect. Propanol still definitely shortens the time of set, although the acceleration is slight. The curves obtained with the different addition agents are still in almost the same order, but again close together. The sorbitol curve almost coincides with that for mannitol.

In Fig. 7, which shows the results at pH 6.6, the order of the curves is completely reversed, it being mannitol, erythritol, glycerol, glycol, methanol,

ethanol, propanol. Furthermore, all are now retarders. The reversed order still obtains at pH 6.1 (Fig. 8), but the individual effects become more divergent, and this divergence increases as the pH is decreased to 5.6 (Fig. 9).
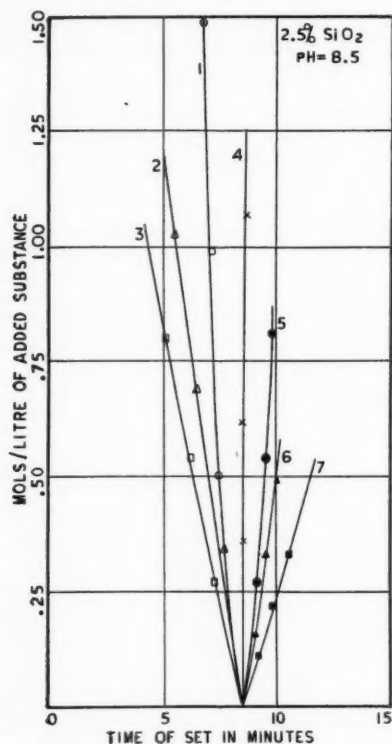

FIG. 5. *Silica gels, initial pH 8.5; 25 cc. of sodium silicate solution + 25 cc. of acid mixture (12.5 cc. of acid + addition agent + water).*
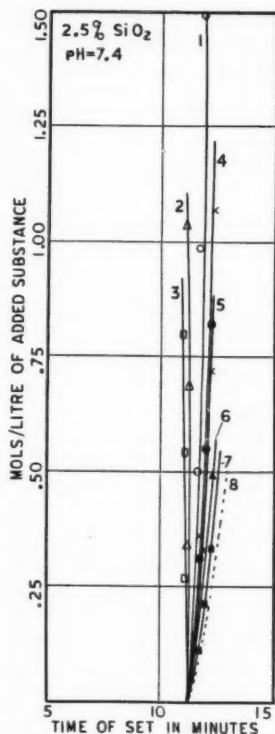
FIG. 6. *Silica gels, initial pH 7.4; 25 cc. of sodium silicate solution + 25 cc. of acid mixture (13.0 cc. of acid + addition agent + water).*

It is known that increasing the concentration of silica decreases the time of set of normal acid and alkaline gels. It might be expected that the effects of concentration and addition agent would be additive. With an accelerator present, an increase in concentration of silica would further decrease the time of set, whereas with a retarder, an increase in concentration of the gel would decrease the effect. This point could not be decided from the writer's previous work because of difference in pH of the gels.

A comparison of Figs. 2 and 6 above would indicate that the effects are not additive.

In order to study the matter further, a series of experiments was performed using '3.35% SiO₂' silicate solution at approximately the same pH as that used in the experiments the results of which are shown in Fig. 8. The curves for this more concentrated gel are given in Fig. 10. Not only was the time of set of the original gel one-half that of the more dilute gel, but the final set with each addition agent was also almost exactly half that observed with the gel prepared from the '2.5% SiO₂' silicate solution. An examination of Figs. 2 and 6 will show that there again the ratio of the times for the different reagents is almost always equal to the ratio of the times for the original gels.
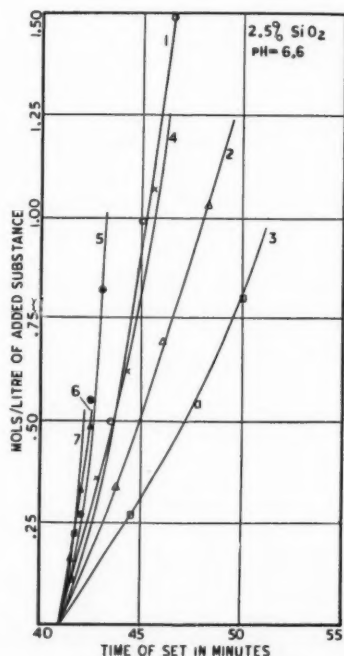

FIG. 7. *Silica gels, initial pH 6.6; 25 cc. of sodium silicate solution + 25 cc. of acid mixture (13.5 cc. of acid + addition agent + water).*

When the pH is plotted against the various times of set expressed as the percentage of the setting times of the original gels, regularities are observed that might not be noticed otherwise. In the range of concentration studied, the percentage effect with addition agent is independent of the concentration of silica, although it is apparent from the data that the actual time of set in minutes varies markedly with the gel concentration. In Fig. 11 the times of set for a constant amount of addition agent (0.5 M) are plotted in this manner. Smooth curves have been drawn from the authors' data, the
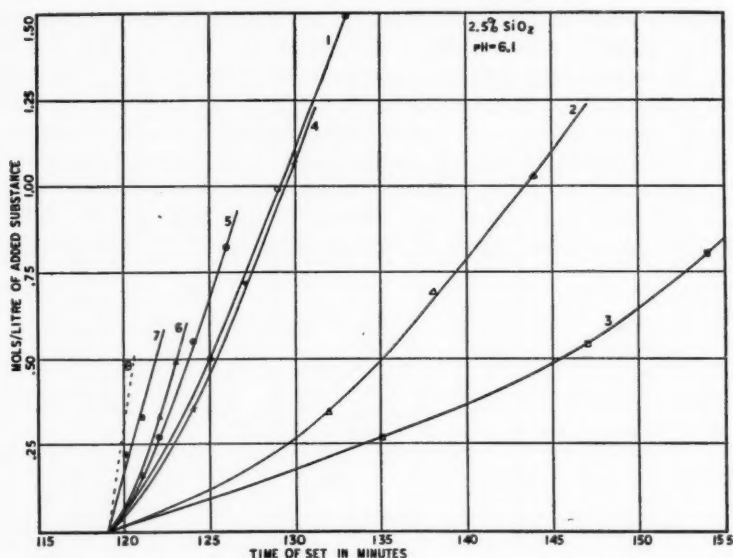
FIG. 8. *Silica gels, intial pH 6.1; 25 cc. of sodium silicate solution + 25 cc. of acid mixture (14.0 cc. of acid + addition agent + water).*
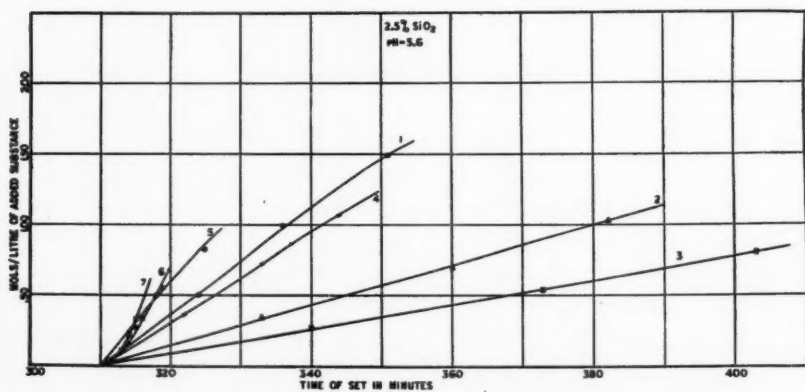

FIG. 9. *Silica gels, initial pH 5.6; 25 cc. of sodium silicate solution (2.5% SiO_2) + 25 cc. of acid mixture (15 cc. of acid + addition agent + water).*

deviations of the calculated points being of the same order as the experimental error. A continuation of the experimental curve for mannitol is given in the insert. The points shown on the figure are those calculated from the results of others as given in Table II. Evidently this treatment can be applied for the comparison of results obtained by different investigators, provided the definition of time of set is the same. The results of Prasad and Hattiangadi

(13), though of the same order, are not strictly comparable, since they used a standard of turbidity as the criterion of set.

TABLE II

Times of set of gels $+ 0.5\, M$ alcohol (t) as percent time of set of standard gel (T) (no alcohol)

0.5 Moles	Silicate solution, '2.5% SiO₂'					
	pH = 9.4	pH = 8.5	pH = 7.4	pH = 6.6	pH = 6.1	pH = 5.6
	t as % *T*					
Methanol	81	89	104	106	105	105
Ethanol	63	85	100	109	113	111
n-Propanol	44	76	99	121	123	119
Glycol	90	100	106	106	105	104
Glycerol	114	112	106	104	105	103
Erythritol	129	119	109	104	103	103
Mannitol	154	133	112	103	102	102

	Silicate solution, '3.35% SiO₂'				Silicate solution, '2.23% SiO₂'		
	*pH = 10.4	*pH = 8.8	pH = 7.4	pH = 6.0	*pH = 10.6	*pH = 8.2	pH = 7.8
Methanol	53	83	105	106	50	95	101
Ethanol	–	–	–	111	–	–	–
n-Propanol	–	–	–	120	–	–	–
Glycol	78	85	105	105	76	103	107
Glycerol	116	109	104	103	120	105	108
Erythritol	141	122	107	103	165	108	111
Mannitol	245	151	110	102	284	120	117

Data by Munro and Alves (9)		Data by Munro and O'Brien (11)		Data by Hurd and Carver (7)	
pH = 10.4; silicate solution, '3.3% SiO₂'		pH = 5.6; silicate solution, '4.4% SiO₂'		pH = 5.5	
Methanol	49	Methanol	107		
Ethanol	24	Ethanol	111	Ethanol	112
n-Propanol	18	*n*-Propanol	122	Glycerol	103
Glycol	77	Glycol	105		
Glycerol	122	Glycerol	104		
pH = 5.1; silicate solution, '3.3% SiO₂'	—	–		—	–
Glycerol	104	—		—	–

Data from (12).

Discussion

Several additional points of interest emerge from a consideration of Fig. 11. The most striking is the convergence of all curves at pH 7. It will also be noted that the point at which the curves coincide is not the 100% line.

In every case the time of set has been lengthened by an amount of approximately 6% by the same number of molecules of addition agent, irrespective of the alcohol used.

Further, the specific effect of the addition agent is greater on the alkaline side. At a pH of two units from the neutral point (pH = 9), the times of set of the alkaline gels vary from 60 to 150% of that of the original gel. On the acid side (pH = 5) the variation lies between 101 and 121%. The effect of the addition agents in the latter case is very slight. In so far as they have been studied, all behave as retarders of gelation.
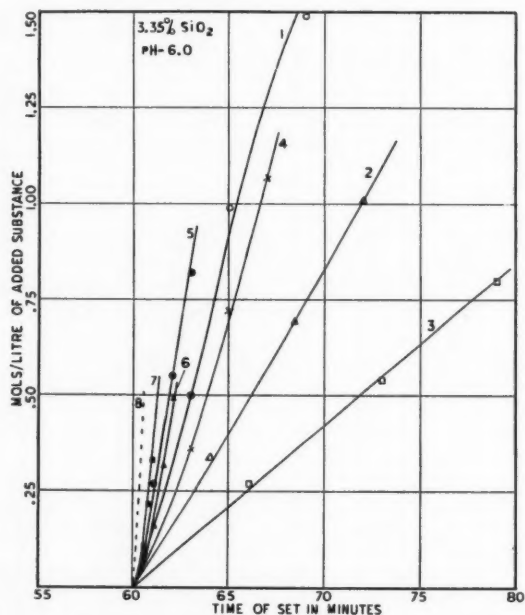

FIG. 10. *Silica gels, initial pH 6.0; 25 cc. of sodium silicate solution (3.35% SiO₂) + 25 cc. of acid mixture (22.0 cc. of acid + addition agent + water).*

The intercepts on the 100% line made by Curves 1 to 4 give the pH at which these alcohols change from accelerators to retarders.

If similar curves were plotted for greater concentrations of addition agent, the curves on the alkaline side would be spread out but would converge at pH 7 at a higher value of the percentage time of set, but Curves 1 to 4 would cut the 100% line at the same pH values. On the acid side, the curves would be displaced to the right. For zero concentration the curve becomes the 100% line.
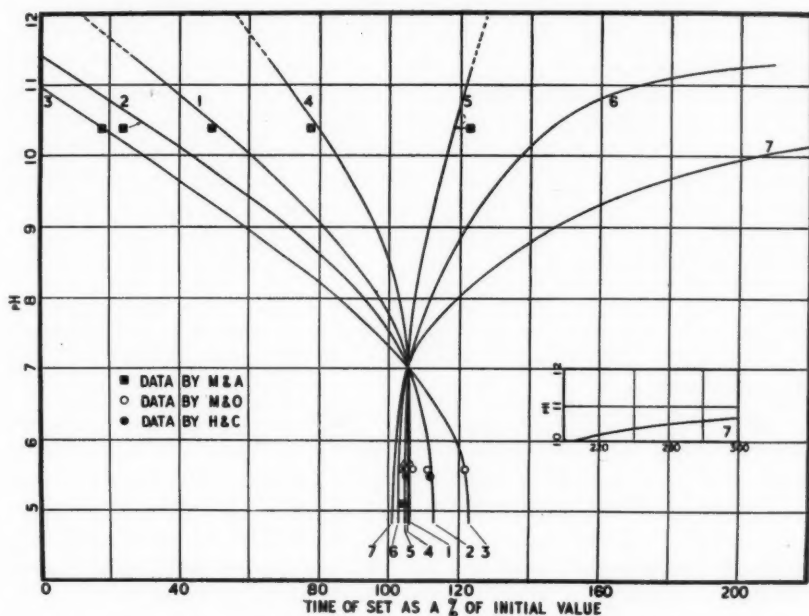
FIG. 11.   *Time of set for gels containing 0.5 moles of different alcohols vs. pH of original gel.*
Solid curves; authors' data.   Points represent data by Munro and Alves,
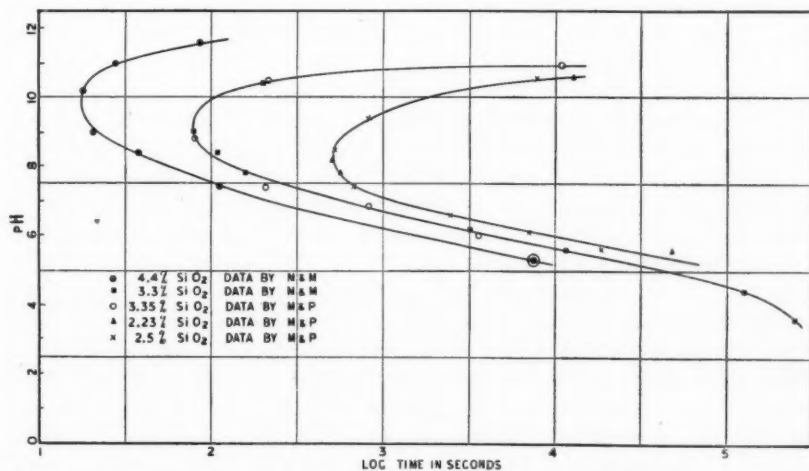*Munro and O'Brien, Hurd and Carver.*

FIG. 12.   *Curves showing pH of gels of minimum times of set for different concentrations of*
silica.   Data by Munro and McNab and present authors.   ⊙ data by Munro and O'Brien.

From the convergence of the curves at pH 7 it is apparent that the dielectric constant of the addition agent plays a negligible part.

In this study the time of set as measured represents the time required for the gel to develop a definite resistance to shear. Fig. 12 shows that when the times for the original gel to reach this constant rigidity are plotted over a range of pH values, the curve passes through a sharp minimum and is symmetrical about this minimum point. The pH at minimum time of set of these original gels increases slightly as the concentration increases.

The points shown on the curve represent data obtained by the authors and others (10, 11). A similar shift was observed by Batchelor (3).

Hurd (6) states that a straight line relation between pH and logarithm of the time of set was obtained with both acid and alkaline gels. Fig. 12 shows that the curve is linear over a portion of the pH range in both acid and alkaline regions.

The points of inflection of the titration curves also show changes comparable to the shift of the pH values at minimum time of set. Further, the point of inflection and the point of minimum time of set are at almost the same pH for the same silicate concentrations.

In view of the shift in gelation curves for original gels as the concentration of silicate is changed, it seems all the more remarkable that the percentage effect of addition agent alone, is virtually independent of the concentration.

Batchelor (3) has summarized various estimates of the isoelectric point of silica sols. These range from pH 4.6 to 6.2. This is not the range showing minimum time of set of the writers' original gels, nor is it the range within which the percentage effect of addition agent is a maximum. The pH at which an addition agent changes from an accelerator of gelation to a peptizing agent or retarder does not coincide with either the point of minimum time of set of the original gel or with the isoelectric point.

Esterification cannot be offered as an explanation of the specific effect of these alcohols. A cursory examination of the data shows a decrease in hydrogen ion concentration of the gelatinizing mixture containing an alcohol. However, a similar change is obtained with other addition agents, e.g., acetaldehyde and acetone (9). Further, the change in pH measured at the time of set and after 24 hr. is the same for the original gel and the gel with addition agents in most cases.

A consideration of the rate constants showed that there would be hardly any esterification during the time of the sol-gel transformation. The reaction might, however, be catalyzed by the presence of SiO_2. A search of the Chemical Abstracts revealed only one reference to silica as a catalyst for esterification. Korolev (8) catalyzed the esterification of β-naphthol and salicylic acid with SiO_2. However, even if equilibrium were reached in this short time the change in pH due to removal of the acetic acid by esterification would be comparable to the change in pH observed immediately on mixing the '3.35% SiO_2' silicate and acid mixture.

Further, the observed pH changes on mixing and after setting of the alkaline gels are much greater than could be obtained by change in acid content due to esterification.   Should esterification occur in the acid gels, the resulting loss of acid should cause, in the time of set of gels containing alcohol, a decrease, rather than the observed increase.   The evidence therefore seems to indicate that esterfication cannot serve as an explanation of the specific behaviour of the alcohols.

It is well known (14, 15) that monohydric alcohols (and other organic substances) are strongly adsorbed by silica gel.   There is evidence (4, p. 563 *et seq.;* 15, pp. 193–198) that colloidal silica and, in fact, even commercial alkali silicates, contain silica particles stabilized by negative hydroxide ions. The adsorption of monohydric alcohols or other addition agent may cause a displacement of a certain number of hydroxide ions and result in a corresponding change in pH.

In a gel, as little as 0.5% of solid matter may immobilize or give a certain amount of rigidity to the 99.5% of dispersion medium.   Gelation must, therefore, be associated with hydration of the particles.   It has been shown by Kruyt (5, p. 78) and others that monohydric alcohols and various other organic materials cause a displacement and removal of the bound water. This would cause an acceleration of the rate of gelation.   Adsorption is known to vary with hydrogen ion concentration, and the magnitude of the effect on the time of set would vary with the pH.   However, this change in pH does not explain the reversal of the effect of monohydric alcohols and glycol at a definite pH.

Further, although there is little information regarding the dehydrating power of higher alcohols, it is known that glycerol is very hygroscopic.   One would expect, therefore, that glycerol would have a marked accelerating effect.   It is obvious then that here some other factor plays a greater role than dehydration.   It is known that sugars and glycerol (1, p. 922) act as stabilizing and peptizing agents of inorganic particles in colloidal systems and that ethanol behaves similarly in acid media (2, p. 277 *et seq.*).   It may be that with the higher polyhydrics in silica sols the protective action which prevents the formation of the gel network is the determining phenomenon.   This may be true also of monohydric alcohols and glycol in the presence of excess hydrogen ion.

It is obvious that acid gels differ from alkaline gels.   Any theory of gelation must account for this fact.

It is felt that many explanations of the process of setting and the structure of the gel after it has set have been based on incomplete data, and that sufficient experimental data have not yet been obtained to permit a satisfactory explanation of these phenomena.

References

1. ALEXANDER, J. Colloid chemistry. Vol. I. Chemical Catalogue Company, New York. 1926.
2. BANCROFT, W. D. Applied colloid chemistry. McGraw-Hill Book Company, New York. 1932.

3. BATCHELOR, H. W.   J. Phys. Chem. 42 : 575-585.   1938.

4. BOGUE, R. H.   The theory and application of colloidal behaviour.   Vol. 2.   McGraw-Hill Book Company, New York.   1924.

5. FREUNDLICH, H.   New conceptions in colloid chemistry.   Methuen and Company, Ltd., London.   1926.

6. HURD, C. B.   Chem. Rev. 22 : 403-422.   1938.

7. HURD, C. B. and CARVER, D. H.   J. Phys. Chem. 37 : 321-329.   1933.

8. KOROLEV, A.   J. Chem. Ind. (Moscow), 4 : 547.   1927.   *In* Chem. Abstr. 22 : 944.   1928.

9. MUNRO, L. A. and ALVES, C. A.   Can. J. Research, B, 15 : 353-359.   1937.

10. MUNRO, L. A. and McNAB, J. G.   Unpublished data.

11. MUNRO, L. A. and O'BRIEN, L.   Unpublished data.

12. MUNRO, L. A. and PEARCE, J. A.   Can. J. Research, B, 16 : 390–395.   1938.

13. PRASAD, M. and HATTIANGADI, R. R.   J. Indian Chem. Soc. 6 : 991-1000.   1929.

14. WARE, J. C.   The chemistry of the colloidal state.   J. Wiley and Sons, New York.   1936.

15. WEISER, H. B.   Inorganic colloid chemistry.   Vol. 2.   J. Wiley and Sons, New York. 1938.